ELLIPTIC SURFACES AND SOME SIMPLE EXOTIC $\mathbb{R}^4$'S

ŽARKO BIŽACA & ROBERT E. GOMPF

0. Introduction and main results

One of the most surprising developments of 4-dimensional topology has been the discovery of *exotic* $\mathbb{R}^4$ *'s* – smooth manifolds that are homeomorphic to $\mathbb{R}^4$ but not diffeomorphic to it. These manifolds represent a uniquely 4-dimensional phenomenon, in that $\mathbb{R}^n$ cannot admit exotic smooth structures when $n \neq 4$. The phenomenon is intimately connected with both of the major advances that have occurred in 4-manifold theory. Exotic $\mathbb{R}^4$'s result from the fact that high-dimensional techniques can be applied to topological 4-manifolds (as shown by Freedman [11]) whereas such techniques cannot be applied to smooth 4-manifolds (as shown by Donaldson, for example [9]). Two distinct classes of exotic $\mathbb{R}^4$'s have been discovered, corresponding to the two fundamental techniques of high-dimensional topology, and ultimately arising from prescient work of Casson [5]. The first type to be discovered arose from the smooth failure and topological success of the surgery theorem. These exotic $\mathbb{R}^4$'s cannot be smoothly embedded in $\mathbb{R}^4$ (with its usual smooth structure). Subsequently the other class arose from the smooth failure and topological success of the h-cobordism theorem. The fundamentally different nature of these latter examples is evidenced by the fact that these exotic $\mathbb{R}^4$'s all embed in the standard $\mathbb{R}^4$. It is now known that both classes contain uncountably many diffeomorphism types. A more detailed exposition of exotic $\mathbb{R}^4$'s can be found in [17].

Naturally, it seems important to have simple, explicit descriptions of such intriguing manifolds. Unfortunately, the existence proofs referred to above are rather abstract, involving complicated infinite construc-

tions. While it is possible, at least in principle, to write exotic $\mathbb{R}^4$'s as unions of increasing sequences $\{C_k\}$ of compact 4-manifolds, these compact manifolds C_k tend to be quite complicated and hard to specify explicitly. For exotic $\mathbb{R}^4$'s of the first type, the manifolds C_k will be complements of tubular neighborhoods of 2-complexes which are embedded in horrendously complicated ways. For examples of the other type, the manifolds C_k have a simpler general description, but the first Betti numbers typically increase superexponentially with k. For either type of exotic $\mathbb{R}^4$'s, the Betti numbers of the 3-manifolds ∂C_k will typically increase superexponentially.

The main purpose of the present paper is to exhibit some exotic $\mathbb{R}^4$'s which admit simple, explicit descriptions. Such descriptions are necessarily infinite, since no known exotic $\mathbb{R}^4$ admits a finite handle decomposition. In fact, a finite decomposition of an exotic $\mathbb{R}^4$ would provide a counterexample to the smooth Poincaré conjecture in either dimension 3 or 4. Our simplest example of an exotic $\mathbb{R}^4$ is given as the interior of the infinite handlebody shown in Figure 1. Note that the infinite construction is just a single chain of 1- and 2-handles that repeats in a simple way. Below, we will give a different description of this manifold that does not use Kirby calculus. To measure the simplicity of this exotic $\mathbb{R}^4$, note that it can be written as the union of a nested, increasing sequence $\{C_k\}$ where each C_k is a compact 4-manifold homotopy equivalent to a circle, so $b_1(C_k) = b_1(\partial C_k) = 1$. (To verify this, let C_k be the manifold obtained by truncating Figure 1 after the k-th Whitehead link, so that C_6 is the handlebody actually pictured. Without changing the homotopy type of C_k, we may undo the clasp in the rightmost 2-handle. Then all handles cancel except the rightmost 1-handle, and we are left with $S^1 \times B^3$.) We will discuss this phenomenon further in §5, which can be read independently of the rest of the paper. We will show that there is more than one diffeomorphism type of exotic $\mathbb{R}^4$ for which the Betti numbers stabilize in this manner, and we will prove some related results. It is hoped that these simple exotic $\mathbb{R}^4$'s are within the range of explicit computability by geometers or physicists. Elsewhere in the paper, we discuss applications of this work to other phenomena: obstructions to knot slicing (§4), Casson handles, elliptic surfaces, and a homotopy K3 surface of Akbulut.

EXOTIC $\mathbb{R}^4$
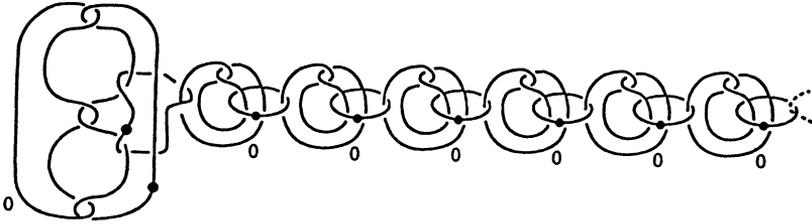
FIGURE 1

Our primary goal is to find simple descriptions of exotic $\mathbb{R}^4$'s. Those which arise from surgery theory are complements of infinite intersections of nested Casson towers. Although such examples can be described explicitly [2], it seems hopeless to attempt to find descriptions simple enough to result in explicit handle presentations. Thus, we focus on those examples which arise from the h-cobordism theorem. Such examples have been studied by DeMichelis and Freedman [7] (see also [19]), who call them *ribbon* $\mathbb{R}^4$'s, since they can be described as follows. Begin with a disjoint collection of *ribbon discs* in the 4-ball B^4, i.e., 2-discs Δ smoothly embedded with $\Delta \cap \partial B^4 = \partial \Delta$ such that the height function (radius) in B^4 is a Morse function on Δ with no local maxima on intΔ. (The latter condition can be dropped with no difficulty.) Remove tubular neighborhoods of these discs from B^4 to obtain a compact 4-manifold called a *ribbon complement*. If we glue 2-handles to the ribbon complement along meridians of the discs, we will recover B^4. If we instead glue Casson handles to these meridians, the resulting interior will be a ribbon $\mathbb{R}^4$. It will be homeomorphic to $\mathbb{R}^4$ since Casson handles are homeomorphic to open 2-handles [11], but it may not be diffeomorphic to $\mathbb{R}^4$. Since any Casson handle embeds in a standard 2-handle, we may also describe this ribbon $\mathbb{R}^4$ as intB^4 minus certain compact subsets of the tubular neighborhoods of the ribbon discs; see below.

The main problem with describing an exotic ribbon $\mathbb{R}^4$ explicitly is in knowing how much complexity is required in the ribbon discs and the Casson handles in order to guarantee exoticness. DeMichelis and Freedman construct exotic ribbon $\mathbb{R}^4$'s using a simply connected h-cobordism between two nondiffeomorphic 4-manifolds. Such examples exist by Donaldson's work [8], [9], and they are topological products by Freedman [11]. The h-cobordism admits a handle decomposition, built on a collar of one boundary component, with only 2-handles and 3-handles. A priori, there is no control over the number of these handles, or of the number of times each 3-handle geometrically runs over each 2-handle. In the resulting exotic $\mathbb{R}^4$ construction, these numbers determine both the number of ribbon discs and the complexity of their linking. In addition, the Casson handles attached to the ribbon complement must embed in a prescribed way in the middle level of the h-cobordism, and the general theory gives no upper bound on the complexity of the Casson handles that may be necessary to accomplish this. Fortunately, Akbulut [1] has produced a nontrivial h-cobordism with a unique 2-handle and 3-handle (which are "π_1-negligible"), and the 3-handle runs only 2 extra times over the 2-handle, the simplest possible situation. It follows that an exotic $\mathbb{R}^4$ can be constructed from just 2 ribbon discs, as described by Figure 2; these are the simplest ribbon discs for the $(-3, 3, -3, 3)$ pretzel link. The first author [3] explicitly determined an upper bound on the complexity of the Casson handles necessary to guarantee exoticness - however, the number of kinky handles of the k-th stage grew according to a superexponential recursive function of k. In the present article, we generalize Akbulut's h-cobordism to obtain a sequence of such simple nontrivial h-cobordisms. By augmenting the proof used by DeMichelis and Freedman with a simple compactness argument, we show that the simplest Casson handle CH^+, with one kink at each stage and all kinks positive, can be used to obtain an exotic $\mathbb{R}^4$, by attaching one copy of CH^+ to each of the two meridians in Figure 2. This is the simplest possible ribbon $\mathbb{R}^4$ of the sort described by DeMichelis and Freedman, and it has the handlebody description shown in Figure 3. However, an additional trick allows us to find an even simpler description of an exotic $\mathbb{R}^4$, namely Figure 1, by eliminating one of the two Casson handles. (The difference of the two Casson handles can be replaced by a standard 2-handle.) Figure 1 represents a ribbon $\mathbb{R}^4$ constructed from the simplest ribbon disc for

the $(-3, -3, 3)$ pretzel knot (Figure 4) by attaching the Casson handle CH^+ to a 0-framed meridian.
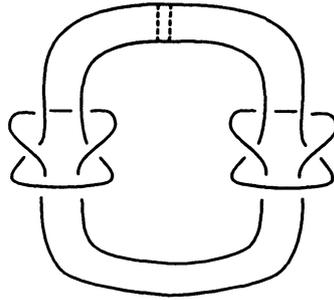
FIGURE 2

EXOTIC $\mathbb{R}^4$
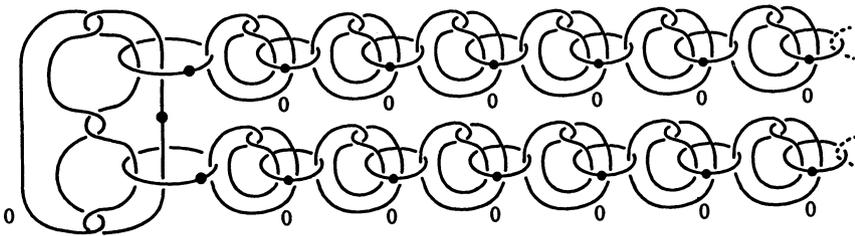
FIGURE 3

To provide an alternate description of these exotic $\mathbb{R}^4$'s that does not explicitly use Casson handles or Kirby calculus, we make a definition. Let ϕ be a smooth embedding from $(D^2 \times D^2, S^1 \times D^2)$ into itself that maps $D^2 \times 0$ onto a disc formed from two oppositely oriented discs $D^2 \times p$ and $D^2 \times q$ by connecting them with a twisted band that runs just beneath $S^1 \times D^2$ as shown in Figure 5, where the band should have a full

left-handed twist.) Any knot K (or link component) in S^3 is represented
by an orientation-preserving embedding $\kappa : S^1 \times D^2 \to S^3$. We use the
0-framing to determine κ, i.e., require that $\kappa(S^1 \times p)$ and $\kappa(S^1 \times q)$ have
linking number 0 in S^3. The composite map $\kappa \circ (\phi | S^1 \times D^2)$ determines
a new knot DK, called the (untwisted, positive) Whitehead double of
K. If K is the boundary of a disc Δ embedded in B^4, then ϕ composed
with the corresponding embedding $\delta : (D^2 \times D^2, S^1 \times D^2) \hookrightarrow (B^4, \partial B^4)$
(with $\delta(D^2 \times 0) = \Delta$) determines a new disc $D\Delta$, called the (positive)
double of Δ. Note that $\partial(D\Delta) = DK$. Clearly we may iterate this
construction using $\phi \circ \cdots \circ \phi$ to define $D^k K = D(D^{k-1} K)$ and $D^k \Delta = D(D^{k-1}\Delta)$ for $k > 1$. (For example, $\phi \circ \phi$ is shown in Figure 6. Note
the twisting in the 0-framing of the original Whitehead curve. This
twisting occurs because the final circle should be unknotted in S^3.)
Note that removing a tubular neighborhood of $D\Delta$ from B^4 is the
same as removing a tubular neighborhood of Δ, and then gluing in the
closure of $D^2 \times D^2 - \text{Im}\phi$. This latter manifold can be shown to be a
closed tubular neighborhood of a disc with one transverse, positive self-
intersection [5]. Thus, removing a neighborhood of $D^k\Delta$ corresponds
to replacing a neighborhood of Δ by the simplest k-stage Casson tower.
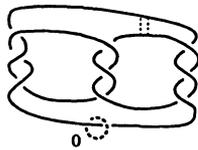
FIGURE 4
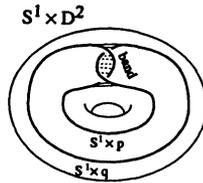
FIGURE 5
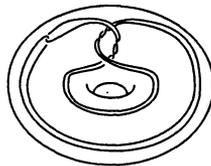
FIGURE 6
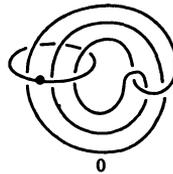
FIGURE 7

Now we can describe ribbon $\mathbb{R}^4$'s as open subsets of B^4. Figure 4 de-

scribes a ribbon disc Δ in B^4, with $\partial\Delta$ given by the $(-3,-3,3)$ pretzel knot. We can see this disc explicitly by considering the intersections of Δ with successively deeper 3-spheres in B^4. Near ∂B^4, each intersection is equivalent to the pretzel knot. Deeper, we pass a saddle point as indicated by the dotted band. The result of this is to cut one of the -3-twisted bands. We are left with a pair of unknotted circles which are unlinked from each other. These circles disappear at local minima, completing the description of Δ. By forming iterated doubles of Δ, we obtain an infinite, nested (decreasing) sequence of embedded copies $\text{Im}(\delta \circ \phi^k)$ of $(D^2 \times D^2, S^1 \times D^2)$ in $(B^4, \partial B^4)$. (To draw these using the correct framings, note the punctured torus visible in Figure 4 as 2 discs connected by 3 twisted bands. The boundary curves should all lie on this torus, except at clasps, where they twist as in Figure 6.) Removing the intersection of these subsets $\text{Im}(\delta \circ \phi^k)$ from B^4, and then removing ∂B^4, we obtain the exotic $\mathbb{R}^4$ of Figure 1 as an open subset of $\text{int} B^4$. (Kirby calculus aficionados can verify that the 3-component link obtained from Figure 1 by deleting all Whitehead links is a handle presentation of the ribbon complement of Figure 4, and that each Whitehead link corresponds to one doubling.) Similarly, Figure 3 is the exotic ribbon $\mathbb{R}^4$ obtained from Figure 2 by iterated doubling of both of the indicated ribbon discs.

In general, for any disjoint collection of ribbon discs in B^4, we can obtain a ribbon $\mathbb{R}^4$ by the above doubling procedure. We can also allow discs with local maxima if desired. The procedure corresponds to adding copies of the simplest Casson handle CH^+ to the ribbon complement. For more general Casson handles, we must precede each doubling by replacing each disc by many parallel copies of itself, and allow doubling using the mirror image of Figure 5. It is worth noting that if the boundaries of the discs form an unlink in ∂B^4, the resulting ribbon $\mathbb{R}^4$ will be diffeomorphic to the standard $\mathbb{R}^4$. (The hypothesis allows us to untwist all of the bands arising from Figure 5 by rotating $S^1 \times p$ parallel to itself through 360^0, so that after the first doubling we are working with a trivial collection of ribbon discs. Thus, we obtain the interior of a single Casson handle. But an easy engulfing argument [11] shows that this is standard.) We are left with some open questions: Which collections of discs in B^4 and Casson handles result in exotic ribbon $\mathbb{R}^4$'s? For example, what if we use CH^+ and the obvious ribbon disc for the square knot? What about CH^+ and the mirror image of

Figure 4? Are two such exotic $\mathbb{R}^4$'s ever diffeomorphic? In particular, what about Figures 1 and 3?

We continue by summarizing our main results. We use a generalization of Akbulut's construction [1] to obtain a sequence of non-product h-cobordisms. The 4-manifolds involved in these constructions are minimal elliptic surfaces, $E(n)$, and their logarithmic 0-transforms, $E(n; 0)$; see §1 for their descriptions. Akbulut's h-cobordism from [1] is between $X \sharp k\overline{\mathbb{CP}}^2$ and $E(2; 0)\sharp k\overline{\mathbb{CP}}^2$, where X is a homotopy K3 surface and k is an arbitrary positive integer. In the present paper we show that the homotopy K3 surface used by Akbulut is the standard K3 surface, that is $X = E(2)$. Furthermore, Akbulut had described the surgery induced by his h-cobordism as the result of deleting a *Mazur manifold* from $X \sharp \overline{\mathbb{CP}}^2$ and then gluing it back by an identification of the boundaries that differs from the initial one by an involution; the Mazur manifold is the contractible manifold described by Figure 7. We generalize Akbulut's construction to obtain an explicit h-cobordism between $E(n)\sharp 2\overline{\mathbb{CP}}^2$ and $E(n; 0)\sharp 2\overline{\mathbb{CP}}^2$, for any integer $n \geq 2$. Each of these cobordisms can also be described as a regluing of the above Mazur manifold by the same involution given in [1].

Lemma 0.1. *For any integer $n \geq 2$ there is an explicitly described (smoothly) non-product h-cobordism $(Z_n^5; \partial_0 Z_n, \partial_1 Z_n)$, such that*

$$\partial_0 Z_n \cong E(n; 0)\sharp_2\overline{\mathbb{CP}}^2 \cong \sharp_{(2n-1)}\mathbb{CP}^2 \sharp_{(10n+1)}\overline{\mathbb{CP}}^2,$$
$$\partial_1 Z_n \cong E(n)\sharp_2\overline{\mathbb{CP}}^2,$$

and Z_n is obtained from $\partial_0 Z_n \times I$ by attaching a single 2-handle and 3-handle. For $n = 2$, this is the cobordism described by Akbulut [1].

Given this explicit description and a procedure for embedding Casson towers [3], a simple compactness argument yields the above-mentioned descriptions of exotic ribbon $\mathbb{R}^4$'s.

Theorem 0.2. *The open handlebody obtained by adding infinitely many open 1- and 2-handles to the open 4-ball as prescribed by Figure 1 or by Figure 3 is an exotic $\mathbb{R}^4$.*

A byproduct of the proof of this theorem is that the involved Casson handle, CH^+, is exotic. We call a Casson handle *exotic* if its attaching circle does not bound a smooth 2-disc in the Casson handle. For an exposition of Casson handles and towers see for example [5] or [19]. Each Casson handle can be described by an infinite based signed tree

([11] or [2]) and when a tree corresponding to a Casson handle is a subtree of another such tree, then the Casson handle with the bigger tree embeds (relative to the attaching areas) in the one with the smaller tree. Consequently, any Casson handle embeds in one with only one kink per level. Note that any Casson handle embedded into an exotic Casson handle has to be exotic itself and so:

Corollary 0.3. ([4]) *Any Casson handle described by a signed tree that contains an infinite positive branch is exotic.*

In [4] it is shown that this result is an easy consequence of L. Rudolph's theorem that no iterated untwisted positive double of a "strongly quasipositive" knot is smoothly slice [21]. The example of a strongly quasipositive knot used in [4] is the positive trefoil T. In this work we generalize Rudolph's result from T to a class of knots that are "greater than or equal to" T. This relation is a generalization of knot concordance from annuli in $S^3 \times I$ to annuli in definite manifolds, and it is due to Cochran and the second author [6]. Here we use a more restrictive condition on the manifold containing the annulus (simple connectedness) and also give the definition in the "negative definite" form.

Definition 0.4. (Compare with Definition 2.1 in [6].) Let K_1 and K_2 be knots in S^3. Then we say that K_2 is *greater than or equal to* K_1, denoted $K_2 \geq K_1$, (or K_1 is *smaller than or equal to* K_2) if there is an embedding A of $S^1 \times I$ into W such that:

 (1) W is a simply-connected, negative definite, smooth, compact 4-manifold,
 (2) $\partial W = \partial^+ W \sqcup \partial^- W = S^3 \sqcup -S^3$ and A restricted to $S^1 \times \{0, 1\}$ gives the knots K_1 and $-K_2$ respectively,
 (3) $[A(S^1 \times I), A(S^1 \times \{0, 1\})]$ is zero in $H_2(W, \partial W)$.

For example, if K_2 can be obtained from a regular projection of K_1 by replacing finitely many negative crossings with positive crossings, then $K_2 \geq K_1$ (Proposition 2.2 in [6]).

Theorem 0.5. (Compare with [21].) *Let K be a knot that is greater than or equal to an iterated, untwisted positive double of the positive trefoil knot, $D^k T$ ($k \geq 0$). Then no iterated, positive untwisted double of K is smoothly slice.*

Rudolph's approach [21] to dealing with iterated doubles is to use Kronheimer and Mrowka [20] to show that a nontrivial "strongly quasipositive" knot such as the positive trefoil cannot be a slice knot, and

that the untwisted, positive double of any strongly quasipositive knot is strongly quasipositive. The relation between strongly quasipositive knots and those greater than or equal to the trefoil is not clear, but we can produce a result combining these notions by inserting our technique for the previous theorem into Rudolph's proof. We obtain:

Theorem 0.6. *Suppose that K and Q are knots with Q nontrivial and strongly quasipositive. If $K \geq Q$, then $D^k K$ is not a slice knot for any $k \geq 0$. Furthermore, the slice genus of K cannot be less than that of Q.*

The rest of the figures are reproduced at the end of this work and they are drawn using Kirby's link calculus [19]. Beside the (by now) standard conventions used to describe 4-dimensional handlebodies and their boundaries, we also use the following convention: if a framed link contains components whose framings are in parentheses, then it represents a 4-dimensional manifold, say M, with two boundary components, denoted by $\partial^- M$ and $\partial^+ M$. The first boundary component, $\partial^- M$, is obtained from S^3 by surgering only the link components with framings in parentheses. The resulting 3-manifold is crossed with a closed interval, i.e., its closed collar is formed. To finish the construction of M, the remaining framed link components are used as instructions for adding 1- and 2-handles to the "upper" side of the boundary of the collar. In the usual setting 1-handles are replaced by 2-handles scooped out from the 0-handle (dotted components of a framed link), but since there is no 0-handle in the case of presence of components with framings in parentheses, the dotted 2-handles are scooped out from the collar. Since $\partial^- M$ is "below" the collar, to obtain its link picture with the orientation induced by M, one has to view the link with framings in parentheses from below or, equivalently, to form its mirror image. (Note that the mirror image of a framing is its negative.) In short, such a framed link represents a cobordism M between $-\partial^- M$, the 3-dimensional manifold obtained from S^3 by surgering the sublink consisting of the components with framings in parentheses, and the 3-manifold $\partial^+ M$, obtained by surgering all components.

1. Handlebody decomposition of elliptic surfaces

Here for each $n \geq 1$ we construct a closed, smooth 4-dimensional manifold M_n and prove that M_n is diffeomorphic to the elliptic surface $E(n)$. An elliptic surface is a compact, complex surface that admits a holomorphic projection onto a compact, connected complex curve such that the generic fibers are elliptic curves; see [18] for more details. For each $n \geq 1$, there is a simply connected minimal elliptic surface, $E(n)$, fibered over the Riemann sphere, with no multiple fibers and with the Euler characteristic $12n$. Minimal here means that it is not a blow-up of some other elliptic surface. Friedman and Morgan [12], [13] have showed that for each n there are infinitely many non-diffeomorphic 4-manifolds that are all homeomorphic to $E(n)$. Due to their large Euler characteristics, elliptic surfaces are hard to deal with directly in terms of handlebodies, although a method for obtaining a handlebody description of an elliptic surface is presented in [18]. A significant simplification in the study of smooth structures on elliptic surfaces is the second author's discovery [15] of the "nucleus" of an elliptic surface. Following the notation from [15], we denote the nucleus of $E(n)$ by N_n and the closure of its complement by Φ_n.

It was shown in [15] that the boundary Σ_n of the nucleus N_n is the Brieskorn sphere $-\Sigma(2, 3, 6n - 1)$, and the complement Φ_n of N_n is the corresponding Milnor fiber. Families of non-diffeomorphic 4-manifolds homeomorphic to $E(n)$ may be constructed by changing the nucleus, for example, by "logarithmic transformations". Since all "logarithmic transforms" of $E(n)$ retain the same complement of their nuclei, Φ_n, any differences among them can be traced to their nuclei. In this work we use only "0-transforms" of $E(n)$, which are known to decompose into connected sums of $\mathbb{C}P^2$'s and $\overline{\mathbb{C}P}^2$'s [15]. The 0-transform of $E(n)$ is denoted by $E(n; 0)$.

Proposition 1.1. (See [15].) *For $n > 1$, the manifolds $E(n)$ and $E(n; 0)$ are not diffeomorphic. Furthermore, if $\hat{W}$ is any closed, simply connected, smooth 4-manifold with negative definite intersection form, then the manifolds $E(n) \sharp \hat{W}$ and $E(n; 0) \sharp \hat{W}$ are not diffeomorphic.*

Proof. It is known ([15, Theorem 6.1]) that the manifold $E(n; 0)$ decomposes into a connected sum of $\pm$ copies of $\mathbb{C}P^2$. Donaldson's theorem B from [9] implies that all Donaldson's polynomial invariants, $q_k(E(n; 0))$, are trivial. Theorem C in [9] implies that $E(n)$ has at least

some nontrivial Donaldson invariants, so $E(n)$ and $E(n;0)$ cannot be diffeomorphic. Proposition (9.3.14) from [10] implies that these Donaldson invariants are stable under forming the connected sum with a negative definite manifold $\hat{W}$, so there is an integer k such that $q_k(E(n)\natural\hat{W}) \neq 0$ and $q_k(E(n;0)\natural\hat{W}) = 0$.   q.e.d.

The simplest elliptic surface $E(1)$ is the complex projective plane blown up 9 times, and it is diffeomorphic to $\mathbb{C}P^2\natural 9\overline{\mathbb{C}P}^2$. For $n > 1$, $E(n)$ may be constructed as a *fiber sum* of $E(n-1)$ and $E(1)$; see for example [16]. The decomposition $E(n) \cong N_n \cup_{\Sigma_n} \Phi_n$ gives a decomposition of the intersection form on $H_2(E(n))$ as

$$(*) \qquad \begin{pmatrix} 0 & 1 \\ 1 & -n \end{pmatrix} \oplus \Big(E_8 \oplus (n-1)(E_8 \oplus 2H)\Big),$$

where

$$H_2(N_n) = \begin{pmatrix} 0 & 1 \\ 1 & -n \end{pmatrix}, \quad H = \begin{pmatrix} 0 & 1 \\ 1 & 0 \end{pmatrix},$$

and E_8 denotes the negative definite symmetric 8 by 8 matrix of the E_8 plumbing.

We start our construction by describing several homeomorphisms between boundaries of 4-dimensional handlebodies. Each of the handlebodies contains a single 0-handle and one or more 2-handles and it is drawn by use of Kirby's link calculus. Each consecutive picture differs from the previous one by a transformation that preserves the boundary. Besides the 2-handles, visible in the figures as framed links, there are some additional link components and framed arcs, drawn with dashed lines and denoted by letters. We will follow their changes under the homeomorphisms.

The first homeomorphism of boundaries that we use is described by Figures 8 – 12 and we denote it by f_n. The next one is denoted by g_n and it is described by Figures 12 – 15. The boundary of the handlebody in Figure 8 is $-\Sigma_n$, the mirror image of the boundary of the nucleus N_n. Figure 9 is obtained from Figure 8 by a -1 blow-up. Figures 10 – 12 are the results of ambient isotopies: First, the outer strand of the doubled unknot in Figure 9 is bent upwards and the result is Figure 10. Then the twist on the 0-framed component is pushed onto the -1-framed component and the arc γ follows the twist, Figure 11. Next, the -1-framed component in Figure 11 is turned into a double of

the unknot by bending forward (towards the reader) the twist and the piece above it. The bent piece forms the the clasp and the inner strand of the -1-framed component in Figure 12. Figure 13 is obtained by introducing a $+1$ blow-up. The new, $+1$-framed circle is slid over the 0-framed circle and the result is Figure 14. Blowing down the $+1$-framed circle produces Figure 15, the final result of $g_n \circ f_n$.

The next homeomorphism of 3-manifolds we will denote by h_k (Figures 16 – 22) and when $k = -1$ it is a well known homeomorphism between the Poincaré sphere ($-\Sigma_1$ in our notation) and the boundary of the E_8 plumbing. This homeomorphism is described in many expositions on Kirby's link calculus (see for example [19]). Here we also follow the changes under the homeomorphism h_k of the four curves denoted by A, B, C and D, and drawn with dashed lines in Figure 16. Figures 17 and 18 are results of the obvious isotopies, Figure 19 is obtained from Figure 18 by a $+1$ blow-up, and two more $+1$ blow-ups produce Figure 20. The next figure is the result of a handle slide, as the arrow in Figure 20 indicates; the $(+1)$-framed circle on the left in Figure 20 is slid over the $(+1)$-framed circle on the right and the arrow indicates the position of the band used in the handle slide. The result is Figure 21. We continue by introducing -1 blow-ups until the framings (3), (2) and $(k+6)$ become $(+1)$, $(+1)$ and $(k+2)$, respectively, then blow down the first $(+1)$ to complete h_k, Figure 22. We add an additional step to this construction and denote the new homeomorphism by h'_n, (Figures 16 – 23). In Figure 23 there are two Hopf links, each with framings 0 and -2. To compensate for the addition of the Hopf links we twist the curve 'B' four times. The twists are indicated in Figure 23 by rectangular boxes, that is, each box should be replaced by two 360^0 positive twists.

Let n be a positive integer greater than one. Figure 24 is a picture of the nucleus N_n with the boundary Σ_n (see [15], Fig. 1). Taking the mirror image of the framed link in Figure 24 defines an orientation reversing homeomorphism of Σ_n onto $-\Sigma_n$, Figure 25. (Note that the mirror image of a framing is its negative.) Figure 25 represents the same handlebody as Figure 8, so we may apply the homeomorphism $g_n \circ f_n$ to its boundary, obtaining Figure 26. We apply the homeomorphism h'_{-1} to Figure 26, with the 0-framed 2-handle corresponding to the circle 'B' in Figure 16, and then blow down the two $(+1)$-framed components to obtain the framed link in Figure 27. We denote this homeomorphism

by ϕ'_n and the 4-dimensional manifold in Figure 27 by W_n. That is, ϕ'_n is a homeomorphism between $-\Sigma_n$ (Figure 25) and $\partial^+ W_n$, the top boundary component of W_n. Note that $\partial^- W_n$, the bottom component of the boundary of W_n is Σ_{n-1}, the boundary of the nucleus N_{n-1} (cf. Figure 25).

If $n = 1$, we define W_1 to be the E_8 plumbing. We start the construction of ϕ'_1 as before using $g_1 \circ f_1$. Since the framing $n - 1$ in Figure 26 is now the 0-framing, we have a 0-framed Hopf link which we can remove. Now we are left only with a -1-framed negative trefoil and we complete the construction of ϕ'_1 by using the above mentioned standard homeomorphism between the trefoil and the boundary of the E_8 plumbing, i.e., Figures 16 – 22, together with blow downs of the two $(+1)$-framed components.

Now we have all the ingredients for our construction of the manifold M_n $(n \geq 1)$. We compose the mirror image homeomorphism from Σ_n onto $-\Sigma_n$ with ϕ'_n, and denote the resulting homeomorphism by ϕ_n. We use the homeomorphism ϕ_n to glue together N_n and W_n over the common boundary, Σ_n. Then we use the homeomorphism ϕ_{n-1} of Σ_{n-1} to glue W_{n-1} onto $\partial^- W_n$. The new boundary is Σ_{n-2} and we repeat the process until we add W_1. The resulting closed 4-manifold, $N_n \cup_{\phi_n} W_n \cup_{\phi_{n-1}} W_{n-1} \cup_{\phi_{n-2}} \cdots \cup_{\phi_1} W_1$, will be denoted by M_n. The complement of N_n in M_n will be denoted by Φ_n, so $\Phi_n = W_n \cup_{\phi_{n-1}} W_{n-1} \cup_{\phi_{n-2}} \cdots \cup_{\phi_1} W_1$. This is consistent with our previous definition of Φ_n, as the next lemma shows.

Lemma 1.2. *For $n > 0$, the above constructed manifold M_n is diffeomorphic to the elliptic surface $E(n)$. Furthermore, the complement of N_n in M_n, $\Phi_n = W_n \cup_{\phi_{n-1}} W_{n-1} \cdots \cup_{\phi_1} W_1$, is diffeomorphic to the Milnor fiber of the Brieskorn sphere $\Sigma(2, 3, 6n - 1)$.*

Proof. We begin by assembling the necessary facts about elliptic surfaces. We construct elliptic surfaces inductively by fiber summing. (See, for example, [16].) That is, for $n > 1$, $E(n) = E(1) \natural_f E(n - 1)$ is formed from the manifolds $E(1)$ and $E(n - 1)$ by removing an open tubular neighborhood of a regular fiber from each, and gluing the complements together along the boundary 3-tori. The gluing diffeomorphism is required to reverse orientation and preserve the structure of the boundaries as $S^1 \times T^2$ determined by the elliptic fibrations. (The identification of each fiber with T^2 may be chosen arbitrarily.) The nucleus N_n of $E(n)$ [15] is obtained from a cusp fiber

union a section by taking a closed regular neighborhood. Throughout this proof, we will denote the closed complement of N_n by Φ'_n. It is shown in [15, Proposition 7.1 and Lemma 3.7] that Φ'_n is diffeomorphic to the Milnor fiber of the $(2, 3, 6n - 1)$ singularity, and that any self-diffeomorphism of $\partial\Phi'_n$ extends over Φ'_n. If we use a regular fiber of N_{n-1} in $E(n-1)$ to form the fiber sum with $E(1)$, we obtain a decomposition of $E(n)$ as $(E(1)\natural_f N_{n-1}) \cup_{\Sigma_{n-1}} \Phi'_{n-1}$. It is easy to see from §7 of [15] that the standard embedding $N_n \subset E(n)$ can be assumed to lie in $E(1)\natural_f N_{n-1}$. In fact, it is formed from a cusp fiber in $E(1)$, together with a section obtained by gluing together sections from $E(1)$ and N_{n-1}. We will denote the closed complement of N_n in $E(1)\natural_f N_{n-1}$ by W'_n, so that $\Phi'_n = W'_n \cup_{\Sigma_{n-1}} \Phi'_{n-1}$. Note that the diffeomorphism type of this union is independent of the choice of the gluing map, since any diffeomorphism of $\partial\Phi'_{n-1}$ extends over Φ'_{n-1}.

It is now sufficient to show that W'_n is diffeomorphic to W_n for each $n > 1$. The lemma will follow immediately: We have a decomposition $\Phi_n = W_n \cup_{\phi_{n-1}} \Phi_{n-1}$ for each $n > 1$. Since $\Phi_1 = \Phi'_1$ (they are both the E_8 plumbing), we will obtain by induction that $\Phi_n = \Phi'_n$ for all n, and so $M_n = N_n \cup_{\Sigma_n} \Phi'_n = E(n)$. Note that the $n = 1$ case, where $M_1 = E(1)$, is already finished.

To begin our proof that $W'_n \approx W_n$, we describe fiber summing in terms of handlebodies. We begin with the nucleus N_{n-1}, which can be obtained from Figure 24 by replacing "$-n$" by "$1-n$". It is easier to see a regular fiber in an equivalent picture, Figure 28. Figure 28 is obtained by replacing each twist in the previous picture (i.e., Figure 24 with $1-n$ instead of $-n$) by a pair consisting of a 1-handle and a -1-framed 2-handle. (Equivalently, canceling the two pairs of complementary 1-and 2-handles in Figure 28 yields Figure 24.) A regular neighborhood of the regular fiber is built from the 0-handle, 1-handles and 0-framed 2-handle. A regular fiber would be visible in Figure 28 as a punctured torus bounded by the 0-framed 2-handle, intersecting (once) the $(1 - n)$-framed circle (which represents a neighborhood of a section) and having the 0-framed meridians to the dotted circles for a symplectic basis of its first homology group (see Figure 31 for the case $n = 2$). A neighborhood of the cusp fiber is obtained by adding the -1-framed 2-handles over the meridians of the dotted circles. Figure 29 represents the dual handlebody of $N_{n-1} - \nu(F)$, that is, the nucleus with an open tubular neighborhood of a regular fiber removed. The open tubular

neighborhood of the regular fiber that we remove consists of a 0-handle, two 1-handles and a (0-framed) 2-handle (a subhandlebody of Figure 28 minus a collar of its boundary), and after they are removed from the nucleus, we are left with (0)-framed Borromean rings in Figure 28, together with three 2-handles, one with framing $1 - n$ and two -1-framed. The dual handlebody is obtained by inverting the boundary (i.e., taking its mirror image) and by adding 0-framed 2-handles to the meridians of the inverted 2-handles [19]; Figure 29 is obtained in this fashion. Figure 30 shows $N_1 \natural_f N_{n-1}$, the result of a fiber sum of the nuclei N_{n-1} and N_1. To $N_{n-1} - \nu(F)$ (Figure 29) we attach $N_1 - \nu(F)$ (Figure 28 with $n = 2$ and with (0)-framings on the Borromean rings) along the common boundary 3-torus. Clearly, this gluing map preserves the $S^1 \times T^2$ product structures, as required.

Next, we draw a link picture of $E(1) \natural_f N_{n-1}$. We describe $E(1)$ by identifying it with $M_1 = N_1 \cup_{\phi_1} W_1$ and drawing M_1 so that a regular fiber is easily visible. To ensure that we use the correct gluing map to construct $E(1) \natural_f N_{n-1}$, we must keep track of the canonical normal framing of the fiber. This will be easy, however, since the fiber will lie in an obvious 3-manifold in each of our pictures, and a normal vector field in the 3-manifold will determine the correct framing. Figure 31 shows the nucleus N_1. The shaded punctured torus together with a core of the 0-framed 2-handle is a regular fiber. Its normal vector field in the boundary of the cusp neighborhood represents the canonical framing. We follow this framed fiber through the homeomorphism ϕ_1 that glues N_1 to the E_8 plumbing, W_1. Figure 32, together with a 4-handle, shows the dual decomposition of the nucleus. Note that the fiber contains the core of a dual 2-handle, corresponding to its intersection with the section. The result of $g_1 \circ f_1$ is Figure 33. We slide the -1-framed curve over the 0-framed curve, so that it becomes a meridian. There is also a Hopf link with (0)-framings in the figure, which we remove to obtain Figure 34. (The torus slides off of the central (0)-framed circle when we slide the 0-framed 2-handle over it.) Now h_{-1} turns the (-1)-framed trefoil into the E_8 plumbing and the result is $E(1)$, Figure 35. Replacing the twists in Figure 35 by Hopf links with a dot and a -1-framing yields Figure 36. In the latter figure, the 0-handle, 1-handles and 0-framed 2-handle comprise a copy of $T^2 \times D^2$ in $E(1)$ such that the core $T^2 \times 0$ with its obvious framing is isotopic to our original framed fiber. Now we perform the fiber sum with N_{n-1}, in

the same way we obtained Figure 30: First, we remove the interior of $T^2 \times D^2$, Figure 37. Then, to the new ∂^--boundary component we glue $N_{n-1} - \nu(F)$, Figure 29, and the result is $E(1)\natural_f N_{n-1}$, Figure 38. Blowing down the two (+1)-framed circles changes the framings of two circles linked with them from (0) to (−1). Then blowing down the latter two circles produces a pair of 0-framed Hopf links. Figure 39 is now obtained by sliding a −2-framed circle off of each Hopf link and then within each Hopf link sliding one circle over the other.

Finally, we show that the nucleus $N_n \subset E(1)\natural_f N_{n-1}$ is visible in Figure 39 as the two 2-handles attached to meridians (with framings 0 and −1) together with the 4-handle. Thus, its complement W'_n is obtained from Figure 39 by erasing the two 2-handles, and it is clearly diffeomorphic to W_n, Figure 27, completing the proof. (It is easy to check directly that Figure 39 represents $N_n \cup_{\phi_n} W_n$, but we must be sure that we have found the correct embedding of N_n, since nonstandard embeddings $N_n \hookrightarrow E(n)$ are known to exist.) Recall that N_n is given by a cusp neighborhood $\nu(C)$ in $E(1)$ together with a section formed by joining sections of $E(1)$ and N_{n-1}. The removal of the cusp neighborhood from $E(1)$ is visible in Figure 32 as the removal of the 4-handle and the 0-framed 2-handle linked with the trefoil. Following this 2-handle through Figures 32 – 35, we see that in Figure 35 it corresponds to the −1-framed 2-handle, and, after the fiber connected sum with N_{n-1} is formed, it corresponds to the −1-framed 2-handle in Figure 39. After we erase this 2-handle, W'_n will be obtained from Figure 39 by removing a disc corresponding to the section of N_n. This disc is the union of a disc in $N_{n-1} - \nu(F)$ with an annulus in $E(1) - (\nu(F) \amalg \nu(C))$. The annulus comes from a disc in $E(1) - \nu(C)$ that is visible in Figure 32 minus the 2-handle linking the trefoil as the cocore of the remaining 2-handle. This becomes the cocore of the 0-framed 2-handle in Figure 36 (minus the −1-framed meridian). When we remove the regular fiber (Figure 37) this becomes an annulus which is "vertical" – it has the form $\mu \times I$ in $T^3 \times I$, where the latter is given by the (0)-framed circles and μ is the obvious meridian. Since the annulus is vertical, we may locate the required disc in $E(1)\natural_f N_{n-1} - \nu(C)$ simply by tracing the disc from $N_{n-1} - \nu(F)$ through our pictures. The latter disc appears in Figure 29 as the cocore of the 0-framed 2-handle linking the $(n-1)$-framed circle. This corresponds to the cocore of the 0-framed meridian in Figure 39. Thus, W'_n is obtained from Figure 39 minus the

-1-framed meridian by deleting the cocore of the 0-framed meridian, i.e., erasing the meridian. We obtain Figure 27, as required.   q.e.d.

2. A family of non-product h-cobordisms

We start by introducing a different handlebody description of the elliptic surface $E(n)$. More precisely, we will use a handlebody description of $N_n \cup_{\phi_n} W_n \cong E(1)\natural_f N_{n-1}$ implicitly described in [1]. This handlebody is obtained by gluing together two manifolds via the three-dimensional homeomorphism described by Figures 40 – 43 and denoted by ψ_n. We will determine the images under ψ_n of the 0-framed meridians to the components of the link, denoted in Figure 40 by β and δ and drawn with dashed lines. In Figure 40 we see a Mazur link whose components have framings -1 and 0. We slide the 0-framed component over the -1-framed component, as indicated by the arrow in Figure 40. As the result we obtain Figure 41. (Note the symmetry that moves δ from one strand of the $+1$-framed component to the other.) Next, we apply h_1 (Figures 16 – 22) with 'B' from Figure 16 being the -1-framed circle, 'C' being the 0-framed circle δ and 'D' (capped off) being β. The result is visible in Figure 42. Then, we blow down the long -1-framed circle in Figure 42, perform four -1 blow-ups and introduce two Hopf links and, after several obvious handle slides, the result is the framed link in Figure 43. This finishes the description of ψ_n.

For $n > 1$, the cobordism Z_n is constructed from three pieces that are h-cobordisms relative to the boundary. The first one was described by S. Akbulut, Figures 45 – 48 in [1]; see also Figures 19 – 37 in [3]. This relative h-cobordism contains a pair of algebraically complementary 2- and 3-handles. The bottom boundary component is denoted by A_0, Figures 44 and 45; Figure 44 is obtained from Figure 45 by canceling the two circles with dots on the right side of the figure. The 2-handle of the h-cobordism is attached to the meridian of the dotted circle on the left of Figure 45. The resulting surgery changes the dot to the 0-framing, and the result "the middle level of the cobordism" $A_{1/2}$ is visible in Figure 46. Attaching the 3-handle to the "middle level" changes the 0-framing of another component into a dot; the result is denoted by A_1, Figure 47. The total result of these two surgeries is that a dot and '0' have exchanged their places. Obviously these surgeries did not disturb

the boundaries, so we have produced an h-cobordism with a product structure over ∂A_0. Note that $\partial A_0 = \partial A_1$ is homeomorphic to the manifold obtained from the mirror image of the link in Figure 40. The manifold in Figure 48 is diffeomorphic to A_1 and Figure 49 is the result of a handle slide. The -1-framed unknotted component unlinked from the other components in Figure 49 represents a copy of $\overline{\mathbb{C}P}^2$ added by a connected sum. So $A_1 \cong Q \sharp \overline{\mathbb{C}P}^2$, where Q is the handlebody resulting from the removal of the -1-framed 2-handle from Figure 49. The dual handlebody decomposition of Q is visible in Figure 50, but a 3- and a 4-handle have to be added to the top. Next, we use the homeomorphism of the boundaries ψ_n to glue A_i, $i = 0, 1$, to the manifold from Figure 51 that we denote by U_n, that is, $\psi_n : \partial A_i \cong \partial^+ U_n$. By taking the product cobordism over U_n, (that is, $U_n \times I$) we have a relative h-cobordism over $A_0 \cup_{\psi_n} U_n$. We have $A_1 \cup_{\psi_n} U_n \cong Q \cup_{\psi_n} U_n \sharp \overline{\mathbb{C}P}^2$, and the manifold $Q \cup_{\psi_n} U_n$ is visible in Figure 52.

Lemma 2.1. *The manifold from Figure 52, together with an invisible 3-handle and a 4-handle,* $Q \cup_{\psi_n} U_n$, *is diffeomorphic to* $E(1) \sharp_f N_{n-1}$.

Proof. Introduce a -1 blow-up to undo a clasp in Figure 52. The result is visible in Figure 53. Doing some obvious handle slides results in Figure 54. Comparing this figure with Figure 30 (in which one has to blow down the two (1)-framed circles) reveals an embedded $N_1 \sharp_f N_{n-1}$ in the manifold from Figure 54. The complement of this embedding is visible in Figure 55. (Blow down the five -1-framed 2-handles that are pieces of the glued nuclei. The (0)-framed unknot from Figure 54 becomes a (+1)-framed unknot. Blowing down this new (+1)-framed circle produces a left hand twist.) We claim that the manifold in Figure 55, together with the invisible 3-handle and the 4-handle, is the E_8 plumbing, which completes the proof. The first step is an application of the "constrained decomposition of E_8" from [3], which we outline next. We start in Figure 55 by sliding the rightmost -2-framed 2-handle over the -1-framed 2-handle. As the result, the handle which we slid is now unlinked from the -1-framed handle, but it changes its framing to -1 and is linked once with the vertically elongated (+1)-framed circle (since it contains a parallel copy of the original -1-framed circle linked with this (+1)-framed circle). Now we repeat the process by sliding the next -2-framed circle off the chain, and again it obtains -1 framing and links

the same $(+1)$-framed circle. We slide the last -2-framed circle 3 times and the result is Figure 56. (Compare with Figures 7 – 18 in [3].) We temporarily disregard the invisible 3- and 4-handle and form a dual handle decomposition of the rest, Figure 57. Then we blow down a small (-1)-framed circle in Figure 57 to obtain Figure 58 and, finally, we blow down all $(+1)$-framed circles and the (-1)-framed circle linked with a 0-framed unknot. The only remaining component with framing in parentheses is now a (0)-framed unknot, so the ∂^--component of the boundary is $S^1 \times S^2$. Finally, we add duals of the 3- and the 4-handle, that is, a 0-handle and 1-handle $(\cong S^1 \times D^3)$, and the result, Figure 59, is the E_8 plumbing. We can obtain this picture of E_8 from the usual one by introducing a canceling pair of 1- and 2-handles, where the 2-handle is a -1-framed meridian to the 2-handle at the end of the longest arm of the E_8 plumbing, and repeating the above procedure to unlink the 2-handles from each other.   q.e.d.

We can now construct the h-cobordisms Z_n described in Lemma 0.1. We have constructed a relative h-cobordism between $A_0 \cup_{\psi_n} U_n$ and $A_1 \cup_{\psi_n} U_n \cong (E(1)\natural_f N_{n-1})\natural\overline{\mathbb{CP}}^2$. We connect together this cobordism with $(\Phi_{n-1}\natural\overline{\mathbb{CP}}^2) \times I$ by gluing them over the common boundary component, $\Sigma_{n-1} \times I$. (The reason for this additional blow-up will be apparent later.) The way we are gluing $\Phi_{n-1}\natural\overline{\mathbb{CP}}^2$ to U_n is via a homeomorphism from $\partial^- U_n$ onto $\partial\Phi_{n-1} = \partial^+ W_{n-1}$ that we denote by ρ_{n-1} and that differs from ϕ_{n-1} by starting with g_{n-1} rather than $g_{n-1} \circ f_{n-1}$. In other words, $\phi_{n-1} = \rho_{n-1} \circ f_{n-1}$. It is easy to see that $Q \cup_{\psi_n} U_n \cup_{\rho_{n-1}} \Phi_{n-1} \cong E(n)$, so the resulting h-cobordism, Z_n, has its upper boundary component, $\partial_1 Z_n := A_1 \cup_{\psi_n} U_n \cup_{\rho_{n-1}} (\Phi_{n-1}\natural\overline{\mathbb{CP}}^2)$, diffeomorphic to $E(n)\natural 2(\overline{\mathbb{CP}}^2)$.

We claim that the other boundary component of Z_n, $\partial_0 Z_n := A_0 \cup_{\psi_n} U_n \cup_{\rho_{n-1}} (\Phi_{n-1}\natural\overline{\mathbb{CP}}^2)$, decomposes as a connected sum of copies of $\mathbb{CP}^2$ and $\overline{\mathbb{CP}}^2$. The lower boundary component of the relative h-cobordism is $A_0 \cup_{\psi_n} U_n$, Figure 60. Note that there is a 4-handle missing from the picture (a dual to the 0-handle in Figure 44), but this time there is no 3-handle involved (the 1-handle in Figure 44 is canceled by the -1-framed 2-handle). To verify that $\partial_0 Z_n$ decomposes, we use the 0-framed 2-handle on the left of Figure 60 to slide all of the 2-handles linked with the (-1)-framed circle off of it. Now the E_7 plumbing linked

with a -1-framed unknot is unlinked from the (-1)-framed circle. It is easy to see that it decomposes into 7 -1-framed 2-handles and a $+1$-framed 2-handle. The remaining piece is Figure 61, which we will glue to Φ_{n-1} via ρ_{n-1}. We cancel the $(n-1)$ and (0)-framed circles in Figure 61 and use the 0-framed 2-handle again to slide the other 2-handles off of the (-1)-framed circle. The result is a connected sum where the first summand comes from a Hopf link with framings $n-2$ and 0 (that is, $S^2 \times S^2$ for n even and $\mathbb{C}P^2 \sharp \overline{\mathbb{C}P}^2$ for n odd) and the other summand is precisely $N_{n-1}(0)$ blown down once (dual to [15], Fig 1). Now the remaining handlebody is the sum of $\overline{\mathbb{C}P}^2$'s and $\mathbb{C}P^2$'s together with $N_{n-1}(0) \cup_{\rho_{n-1}} \Phi_{n-1} \cong E(n-1;0)$. As it was shown in [15, Theorem 6.1], $E(n-1;0)$ decomposes as a connected sum of $\mathbb{C}P^2$'s and $\overline{\mathbb{C}P}^2$'s.

To complete the proof of Lemma 0.1 we have to show that our construction for $n = 2$ is identical to Akbulut's [1]. That is, our cobordism Z_2' obtained from Z_2 by removing the last $\overline{\mathbb{C}P}^2$ summand is diffeomorphic to Akbulut's h-cobordism Z_A. First, we show that our $U_2 \cup_{\rho_1} \Phi_1$ is diffeomorphic to Akbulut's M_1. The constructions are easily compared using [1, Figure 23] and our Figure 51. The subsequent part of both constructions is gluing of an E_8 plumbing. In our construction we first use the homeomorphism g_1 (Figures 12 – 15). This homeomorphism changes the framings of the components linked with the (0)-framed circle in Figure 51: the (1)-framed circle obtains (0)-framing and the -1-framed circle becomes a -2-framed circle. Now we have a Hopf link with (0)-framings that we can remove from the picture. The new picture differs from [1, Figure 23] in the trefoil having (-1)-framing instead of the $+1$-framing and in having two more -1-framed meridians. We continue with the standard homeomorphism that turns the trefoil into the boundary of the E_8 plumbing. Continuing the construction in [1] we notice that the $+1$-framed trefoil in [1, Figure 23] becomes an E_8 plumbing with two extra -2-framed components. It is easy to see that the resulting handlebody does not depend on the precise stage of the construction where the component visible in [1, Figure 23] as a trefoil was blown-up twice. Therefore, both constructions produce the same manifold, $M_1 \cong U_2 \cup_{\rho_1} \Phi_1$. Now $\partial_0 Z_A$ is obtained by attaching a 2-handle along the 0-framed curve α in [1, Figure 23] which is the same as our β, so the diffeomorphism $U_2 \cup_{\rho_1} \Phi_1 \cong M_1$ extends to

$\partial_0 Z_2' \cong \partial_0 Z_A$. Similarly, Akbulut attaches the contractible manifold which we call Q by gluing a 2-handle along the $+1$-framed ellipse in [1, Figure 37] (which we will call σ), together with a 3- and 4-handle. The latter figure can be transformed into our Figure 41 by blowing up once to remove a twist from the twisted band and reduce the framing on σ by one. Then σ corresponds to our curve δ. Thus, Akbulut's homotopy K3 surface, $X = Q \cup_\partial M_1$, is diffeomorphic to $E(2)$, and $\partial_1 Z_A = X \sharp \overline{CP}^2$ is diffeomorphic to $\partial_1 Z_2'$. Since the diffeomorphisms $\partial_i Z_A \cong \partial_i Z_2'$ commute with the obvious homotopy equivalences, it follows by high-dimensional surgery that $Z_A \cong Z_2'$.

3. Ribbon $\mathbb{R}^4$'s

The non-product part of the h-cobordism Z_n contains the same rel ∂ h-cobordism between A_0 and A_1 that was described in [1] and that was used in [3] to embed a ribbon $\mathbb{R}^4$. In Figures 45 – 47 we can see embeddings of the handlebodies from Figures 62 – 64, each embedding into one of the levels of the cobordism Z_n. Note that if the standard 0-framed 2-handles were attached onto the dashed circles, then the resulting manifolds in Figures 62 and 64 would be 4-balls, and the one in Figure 63 would turn into a punctured $S^2 \times S^2$. If one could add these 2-handles ambiently, in an appropriate level of the cobordism, then by use of the Whitney trick Z_n will obtain a product structure (compare with [7] or [3]). As shown in [3], the dashed circles in Figures 62 – 64 are capped by twice-punctured discs, smoothly embedded in ∂A_0, $\partial A_{1/2}$ or ∂A_1, respectively. These punctured discs are described in [3, Figures 38 – 44] which are the mirror images of the actual manifolds. (We use the 2-handles on the right of Figure 47 to cancel two 1-handles. The dashed circles will then be parallel, but with a -1-twist between them and -1-framings. Each one obviously bounds a disc that is twice-punctured by the circle with a dot.) Since Q was glued to U_n by a homeomorphism that includes taking a mirror image (Figures 49 and 50), the punctures are isotopic to the meridian β in Figure 40; two of the punctures are unlinked with 0-framing and two come linked and with $+1$-framings, exactly as in Figure 44 from [3]. The meridian β in $\partial^+ U_n$ can be connected by an embedded annulus in U_n to $\partial^- U_n$. As explained in [3], the two $+1$-framed meridians bound an embedded pair

of discs, namely copies of the core of one of the -1-framed 2-handles from Figure 51 ; see Figure 60 in [3]. The remaining two meridians are 0-framed isotopes of β in Figure 51 ; see Figure 43. We show that each copy of the 0-framed meridian β bounds a Casson tower embedded into $\Phi_{n-1} \natural \overline{\mathbb{C}P}^2$. It suffices to assume that n is large.

Now $\Phi_{n-1} = W_{n-1} \cup_{\phi_{n-2}} W_{n-2} \cup_{\phi_{n-3}} \cdots \cup_{\phi_1} W_1$, and we start our description with W_{n-1} on the top, Figure 65. Before we glue W_{n-2} to $\partial^- W_{n-1}$, we will change the handlebody representing W_{n-1}. Figure 66 is the result of two handle slides in Figure 65. In Figure 67 we introduce a pair of complementary 1- and 2-handles (the 2-handle comes with a -1-framing). Next, "the constrained decomposition of E_8" from [3] is used to obtain Figure 68 ; cf. the proof of Lemma 2.1. We want to follow the curve denoted by β in Figures 40 – 43 in Φ_{n-1}. Since Φ_{n-1} was glued to $\partial^- U_n$ via ρ_{n-1}, we see β as 'D' in Figures 16 – 23, but, of course, as a closed unknotted curve, and so it is a meridian to the $(k+2)$-framed unknot in Figure 23. Therefore, β is the meridian to the 1-handle in Figure 68. Figures 69 – 74 are results of handle slides. Next, we apply ϕ_{n-2} to $\partial^- W_{n-1}$, that is we transform the (0)- and $(n-2)$-framed components according to Figures 8 – 23 , and the result is Figure 75.

We will embed a compact handlebody, by discarding certain 2-handles from Φ_{n-1}: in Figure 75 we will discard the $+1$-framed 2-handle and also the two -1-framed 2-handles that are linked with both the dotted circle on the left and the long 0-framed 2-handle. The result is visible in Figure 76. Note that the nine -1-framed 2-handles linked with the dotted circle can be slid over the 0-framed 2-handle, so that now they are linked with the longer $(+1)$-framed circle on the right. Next, we cancel the 1-handle (dotted circle) and the 0-framed 2-handle. The remaining handlebody is W_{n-2} with nine additional 2-handles attached to -1-framed meridians. We iterate our construction with this new handlebody in place of W_{n-1}, in order to attach the next level, W_{n-3}. This time, Figure 65 has nine additional -2-framed circles (and n replaced by $n-1$). Following the circles through Figures 65 – 75 we obtain nine extra -1-framed meridians to the dotted circle in Figure 75. We again discard a $+1$ and two -1-framed 2-handles. Continuing in this fashion, until W_1, we obtain a subhandlebody of Φ_{n-1} that is visible in Figure 77. (Note that on the bottom level we do not have pairs of Hopf

links and that we have retained the connecting +1-framed 2-handle.
Also, we perform the "constrained decomposition of E_8", so instead of
eight −2-framed 2-handles we now have a 1-handle, eight −1-framed
2-handles and a +1-framed 2-handle.) After removing one more han-
dle and a handle slide we have the manifold in Figure 78. Note that
there are $9(n-1)-1$ many −1-framed meridians to the dotted circle in
this picture, and we obtain Figure 79 by removing one of these meridi-
ans. An ambient isotopy together with a blow-up produces Figure 80.
Note that the role of the blow-up was to change the +1-framing into a
0-framing.

Next, we utilize a configuration introduced in [3], that turns −1-
framed circles to levels of a Casson tower. The process is illustrated
in Figure 81. The union of the core of the 0-framed 2-handle and the
surface visible in Figure 81 produces a punctured torus, T^2. Taking
parallel copies of the core of the 0-framed 2-handle and then adding
obvious punctured tori to its boundary produces arbitrary many dis-
joint copies of T^2, each having a single puncture γ that is a meridian
to the dotted circle. As the figure indicates, there is a symplectic ba-
sis of $H_1(T^2)$ consisting of two 0-framed circles, denoted by μ and λ.
Note that both μ and λ are ambiently isotopic to β. We surger each of
the tori by two copies of a core of a −1-framed 2-handle that is linked
with the dotted circle. More precisely, we delete from T^2 a regular
neighborhood of the circle μ. The resulting new boundary components
are two unlinked meridians to the dotted circle. The boundaries of
the two copies of the core of a −1-framed handle are linked once and,
since we are using opposite orientations for the copies of the core, their
linking number is +1. To connect an unlink with a Hopf link by a
pair of pipes, we obviously have to introduce an intersection between
the pipes. The result of this construction is an immersed disc with
boundary γ equal to a 0-framed meridian to the dotted circle and with
a single self-intersection point with a positive sign. A regular neigh-
borhood of the resulting disc is a kinky handle whose attaching circle
is the 0-framed meridian γ to the dotted circle. In order to produce
two Casson towers from these kinky handles, we also have to identify
a *standard loop* for each self-intersection, namely, a framed loop that
passes through the self-intersection point and on which we can attach
the next level. In Figure 81 the standard loop is isotopic to the curve
λ: the self-intersection is an intersection between the two pipes that

we may as well assume to be between the two copies of the curve μ. The rest of the loop has to be in the complement of μ and the defining property of a standard loop is that a surgery on it by an embedded disc will result in an embedded 2-disc whose regular neighborhood is a 2-handle with the same framing on the boundary. The loop λ has the required properties. In Figure 81, λ has the 0-framing as determined by the torus, and it is linked once with the dotted circle. As it was explained in [3], the regular neighborhoods of immersed discs that were obtained by using a different -1-framed 2-handle for each, can be "piped together" to form a Casson tower that has only one kink per level and whose kinks are all positive. (This is because λ and γ are isotopic framed curves.) The number of levels of such a Casson tower we can construct is bounded by the number of available -1-framed 2-handles that are linked with the dotted circle. The "tower factory" can produce a total of $9n - 11$ kinky handles. These can be connected by pipes to form two Casson towers with $\left[\frac{9n-11}{2}\right]$ levels on each. Thus we have extended the embedding of the handlebody in Figure 62 to the one in Figure 3, where only the first 6 levels of the Casson towers are visible. Note that decomposing the manifold U_n in Figure 51 would allow us obtain a few more levels of kinky handles, but we are interested only in the fact that the number of levels of the embedded Casson towers tends to infinity when n is increased.

Proof of Theorem 0.2.   Let us denote by R the open 4-manifold obtained by attaching a copy of the Casson handle CH^+ to each dashed circle in Figure 62 and then removing the boundary. The resulting (infinite) framed link picture is indicated in Figure 3 where two chains of Whitehead links have to be infinite. Since each Casson handle is homeomorphic to the standard open 2-handle [11], our manifold R is clearly homeomorphic to $\mathbb{R}^4$. Let us suppose that R is diffeomorphic to $\mathbb{R}^4$. There is an increasing sequence of embedded compact manifolds with boundary in R, namely for each $k \geq 0$ we attach two k level Casson towers to the handlebody from Figure 62. We denote this compact manifold by C_k and arrange that $C_k \subset \text{int} C_{k+1}$. Since we have assumed that R is standard, C_0 can be engulfed by B_0^4, a smooth 4-ball whose boundary is a smoothly embedded 3-sphere, S_0^3. Since $R = \bigcup_k C_k$ and B_0^4 is compact, there is an integer $k \geq 1$ such that B_0^4 is contained in C_k. For n large enough C_k is embedded in both $\partial_1 Z_n \cong$

$E(n) \sharp 2\overline{\mathbb{CP}}^2$ and $\partial_0 Z_n \cong E(n; 0) \sharp 2\overline{\mathbb{CP}}^2$. As argued in [7] and [19] the h-cobordism above the complement of C_0 in $\partial_0 Z_n$ has a product structure. This product structure lifts S_0^3 from $\partial_0 Z_n$ into S_1^3, a 3-sphere in $\partial_1 Z_n$. Then, an argument from [19] shows that S_1^3 has to bound a standard 4-ball in $\partial_1 Z_n$. Therefore, the product structure over $\partial_0 Z_n - \text{int} B^4$ can be smoothly extended over the 4-ball. Since $E(n) \sharp 2\overline{\mathbb{CP}}^2$ is not diffeomorphic to $E(n; 0) \sharp 2\overline{\mathbb{CP}}^2$, we have a contradiction. Therefore, R is an exotic $\mathbb{R}^4$.

The same argument can be used to show that the open infinite handlebody in Figure 1 is an exotic $\mathbb{R}^4$: note that the embeddings of the handlebody in Figure 62 into $\partial_0 Z_n$ and $\partial_1 Z_n$ can be expanded to embeddings of the handlebody in Figure 82; see Figures 45 and 47. By canceling a pair of 1- and 2-handles we obtain Figure 83. Increasing n and adding Casson towers with increasing numbers of levels again produces an increasing family of of compact manifolds that do not contain an embedded smooth 4-ball. Their union, our ribbon $\mathbb{R}^4$ from Figure 1, is therefore exotic.   q.e.d.

4. Non-sliceness of untwisted, positive doubles

We have embedded a k level Casson tower into $\Phi_{n-1} \sharp \overline{\mathbb{CP}}^2$, for any fixed $k > 0$ and sufficiently large n, and the "standard framed loop" on each level is visible in Figure 81 as the 0-framed curve λ. On the top level of the Casson tower we may slide λ over one of -1-framed meridians of the dotted circle, i.e., we cap λ by the core of a -1-framed 2-handle. Although the standard framed loop λ now bounds an embedded 2-handle, the attaching was performed with an incorrect framing, -1 instead of 0 (with respect to the orientation in Figure 81).

Recall that a link calculus picture of the k level Casson tower with only one positive kink per level, is a Hopf link with one component doubled k times. One of the components is a dotted circle and the other is the 0-framed attaching circle, doubled k times; see [5] or [11]. In this picture, "the standard framed loop" is a 0-framed meridian to the dotted circle. In other words, adding a 0-framed 2-handle over this loop would produce a 2-handle as the resulting total manifold and with unchanged framing of the attaching area (the dotted circle disappears from the picture). We attach a 2-handle over this "standard framed

loop", but with -1 framing. The result is still a 4-ball (the dotted unknot disappears), but the k times doubled attaching circle obtains a -1 twist and becomes a $k-1$ times doubled positive trefoil, $D^{k-1}T$.

We can now prove Theorem 0.5. We have obtained an embedding of an annulus into $\Phi_{n-1}\sharp\overline{\mathbb{CP}}^2$ with the interior of the 0-handle removed such that one end of the embedded annulus is the 0-framed circle denoted by β in Figure 75, and the other end is $D^{k-1}T$ in the boundary of the 0-handle. Suppose that a knot K is greater than or equal to $D^{k-1}T$, in the sense of Definition 0.4. That means that an annulus A, embedded in a negative definite manifold W, connects these two knots. Glue a 4-ball over the component of the boundary of W that contains K, and identify the other component with the boundary of the removed 0-handle in $\Phi_{n-1}\sharp\overline{\mathbb{CP}}^2 - \mathrm{int}B^4$. If the knot K were slice, we could use the union of a slicing disc (in the 4-ball added to W), an annulus in W (from Definition 0.4) with $D^{k-1}T$ on the other end and then with an annulus with the circle 'β' on the other end. The resulting disc would be a slicing disc for β inside $\Phi_n\sharp\overline{\mathbb{CP}}^2\sharp\hat{W}$, where $\hat{W} = W \cup_{\partial W} 2(B^4)$, and the disc would induce the 0-framing on β. Since β is a puncture on each of the embedded punctured Whitney discs, its sliceness would imply the existence of smoothly embedded Whitney discs and a smooth product structure on the h-cobordism Z_n. That would result in a diffeomorphism between $E(n)\sharp 2\overline{\mathbb{CP}}^2\sharp\hat{W}$ and $E(n;0)\sharp 2\overline{\mathbb{CP}}^2\sharp\hat{W}$, which is impossible by Proposition 1.1.

To complete the proof of Theorem 0.5, it suffices to prove the non-sliceness of iterated doubles of knots greater or equal to an iterated double $D^\ell T$ of the positive trefoil. This statement follows from Proposition 2.7 in [6], that is, forming satellites preserves the "$\le$" or "$\ge$" relation. Specifically, suppose that a knot K is greater than or equal to $D^\ell T$. Then for any k, $D^k K$ is greater than $D^{k+\ell}T$. We have already shown that such a knot cannot be slice.   q.e.d

Proof of Theorem 0.6. We are given knots K and Q with Q nontrivial and strongly quasipositive and $K \ge Q$. We will show that the slice genus of K can not be less than that of Q. (The slice genus of K is the minimal genus of an orientable surface in B^4 with boundary K. Note that this is zero if and only if K is slice.) Since $D^k K \ge D^k Q$ and the latter is also strongly quasipositive and not slice [21], it will immediately follow that $D^k K$ is not slice for any $k \ge 0$. Rudolph shows

that there is a 4-ball B embedded in $\mathbb{C}^2 \subset \mathbb{C}P^2$ and a smooth complex curve $C \subset \mathbb{C}P^2$ transversely intersecting ∂B, with $C \cap \partial B = Q$, and that $C \cap B$ realizes the slice genus of Q. Suppose that the slice genus of K were smaller then this. As in our previous proof, we could replace int$B$ by a negative definite manifold to obtain a closed manifold $\mathbb{C}P^2 \natural \hat{W}$ containing a surface S representing the homology class determined by C, but with the genus of S less than that of C. As in Kronheimer and Mrowka [20], we take the double branched cover along a generic sextic curve near the line at infinity in $\mathbb{C}P^2$. The curve C lifts to a smooth holomorphic curve $\tilde{C}$ in K3. Similarly, S would lift to a surface $\tilde{S}$ in K3$\natural\hat{W}\natural\hat{W}$. It is easily checked that $\tilde{S}$ would represent the homology class determined by $\tilde{C}$, but its genus would be smaller, contradicting Theorem 1.1 of [20]. (The curve $\tilde{C}$ minimizes genus in K3 since it is holomorphic and $c_1(\text{K3}) = 0$. The negative definite summands cause no complications.)

5. Remarks on exotic $\mathbb{R}^4$'s

In this section, we define an invariant that measures the complexity of the end of an exotic $\mathbb{R}^4$. We show that, as measured by this invariant, the examples constructed in this paper are particularly simple. We prove that there is more than one diffeomorphism type of such simple exotic ribbon $\mathbb{R}^4$'s. Then we show how to fit these examples into a family of $\mathbb{R}^4$'s that is naturally indexed by a 2-dimensional set such that each uncountable subset represents uncountably many diffeomorphism types.

First, we recall the operation of *end-summing*. Given two exotic $\mathbb{R}^4$'s, R_1 and R_2, we glue them together "at infinity" as follows. Choose proper embeddings $\gamma_i : [0, \infty) \to R_i$, $i = 1, 2$, and then glue both R_1 and R_2 to $[-1, 1] \times \mathbb{R}^3$, by identifying $(0, 1] \times \mathbb{R}^3$ with a tubular neighborhood of γ_1, and $[-1, 0) \times \mathbb{R}^3$ with a tubular neighborhood of γ_2 (preserving orientations). It can be shown that this is a well defined operation on diffeomorphism types and extends to a commutative and associative operation on countable collections of diffeomorphism types. The end-sum of R_1 and R_2 is denoted by $R_1 \natural R_2$, and the end-sum of k copies of R (allowing $k = \infty$) is denoted by $\natural_k R$. See [14] for further details.

Now we define an invariant. Let R be a possibly exotic $\mathbb{R}^4$. For any compact subset C of R, there is a smooth compact 3-manifold in $R - C$ that separates C from infinity, for example, pull back a sufficiently large regular value of a proper map of R into $[0, \infty)$. Let b_C denote the minimum over all such 3-manifolds of the first Betti number. Clearly, for $C \subset C' \subset R$ we have $b_C \leq b_{C'}$.

Definition 5.1. The *engulfing index* $e(R)$ is the supremum of $\{b_C | C \subset R\}$.

This is either infinite or a nonnegative integer. Note that $e(R)$ only depends on the end of R; in fact, it can be just as easily defined for any isolated end of a smooth manifold. For end-sums, $e(\natural R_i) \leq \sum e(R_i)$.

Some of the known exotic $\mathbb{R}^4$'s are constructed so that sequences of 3-manifolds $M_i \subset R$ are explicitly produced (up to ramification) for which any compact $C \subset R$ is separated from infinity by some M_i. However, in all previously known cases, the first Betti numbers increase rapidly as i increases, due to the presence of increasingly complicated Casson tower boundaries in the 3-manifolds. It seems reasonable to conjecture that all exotic $\mathbb{R}^4$'s arising from surgery theory have infinite e, as do those arising from the h-cobordism theorem without careful attention to ramification of the towers. However, a brief look at Figures 1 and 3 shows that these exotic $\mathbb{R}^4$'s have finite e.

Proposition 5.2. *For R as in Figure 1, $e(R) \leq 1$. For R as in Figure 3, $e(R) \leq 2$.*

Note, however, that even though the obvious 3-manifolds have constant b_1, there is still a sense in which the 3-manifolds become increasingly complex towards infinity. Namely, the number of incompressible tori increases without bound. (The torus decompositions contain an increasing number of Whitehead link complements.) It seems reasonable to conjecture that for R as in Figure 1, $e(\natural_\infty R) = \infty$. It would follow that $e(R) = 1$, and that the manifolds $\natural_k R$, $k = 0, 1, 2, \ldots, \infty$ realize all possible values of e (since any compact subset of $\natural_\infty R$ lies in some $\natural_k R$, with k finite), so they must all be distinct. (If $\natural_{k_1} R \cong \natural_{k_2} R$ for $k_1 \neq k_2$, then $\{\natural_k R\}$ represents only finitely many diffeomorphism types.) On the other hand, it seems difficult to rule out the possibility that each $\natural_k R$ ($k \geq 1$) could be diffeomorphic to R. Thus, to prove that there is more than one exotic $\mathbb{R}^4$ with finite e, we need a different approach.

To proceed further, we define some equivalence relations.

Definition 5.3. Let X be a compact 4-manifold. Two manifolds R_1 and R_2 homeomorphic to $\mathbb{R}^4$ will be called X-stably diffeomorphic if $R_1 \natural_\infty X$ and $R_2 \natural_\infty X$ are diffeomorphic.

Here we take connected sums with infinitely many copies of X along any properly embedded, infinite collection of 4-balls in R_i. The sum is easily seen to be independent of the choice of the collection of 4-balls. Since R_1 and R_2 must be properly h-cobordant, they are necessarily $S^2 \times S^2$-stably diffeomorphic. Similarly, they are $\mathbb{C}P^2 \natural \overline{\mathbb{C}P}^2$-stably diffeomorphic. For any fixed X, if R_1 and R_2 are X-stably diffeomorphic and so are R_3 and R_4, then $R_1 \natural R_3$ and $R_2 \natural R_4$ will be X-stably diffeomorphic (and similarly for infinite end-sums).

Proposition 5.4. *Let R be as in Figure 1 or Figure 3. Then R is $\mathbb{C}P^2$-stably diffeomorphic to $\mathbb{R}^4$, but not $\overline{\mathbb{C}P}^2$-stably diffeomorphic to $\mathbb{R}^4$. In fact, for any simply connected negative definite X, R will not be X-stably diffeomorphic to $\mathbb{R}^4$.*

Corollary 5.5. *The manifolds $\mathbb{R}^4$, R, $\bar{R}$ (= R with reversed orientation) and $R \natural \bar{R}$ all represent distinct oriented diffeomorphism types of ribbon $\mathbb{R}^4$'s with finite engulfing index e.*

Proof of Proposition 5.4. We work with Figure 1; a similar proof applies to Figure 3. To prove that R is $\mathbb{C}P^2$-stably standard, we let C_k denote the ribbon complement union the first k stages of the Casson handle, i.e., Figure 1 cut off after k Whitehead links. Using collars of the boundaries, we may arrange that $C_k \subset \text{int} C_{k+1}$ for each k, and that R is the union of the compact manifolds C_k. Let $\hat{C}_k = C_k \natural_k \mathbb{C}P^2$, so that $\hat{C}_k \subset \text{int} \hat{C}_{k+1}$ and $\cup \hat{C}_k = R \natural_\infty \mathbb{C}P^2$. For any fixed k, we may use the $\mathbb{C}P^2$-summand of $\hat{C}_{k+1} - \hat{C}_k$ to remove the positive self-intersection of the core of the top stage kinky handle of $\hat{C}_{k+1}$ without changing its framing. We obtain a submanifold $B_k = \hat{C}_k \cup$ 2-handle in $\text{int} \hat{C}_{k+1}$. But B_k is diffeomorphic to $B^4 \natural_k \mathbb{C}P^2$. Since $B_k \subset \text{int} B_{k+1}$ for each k, it is easy to construct a diffeomorphism from $R \natural_\infty \mathbb{C}P^2 \approx \cup B_k$ to $\mathbb{R}^4 \natural_\infty \mathbb{C}P^2$.

To prove the rest of the proposition, we repeat our proof that R is exotic, summing with copies of X whenever necessary. We assume that $R \natural_\infty X$ is diffeomorphic to $\mathbb{R}^4 \natural_\infty X$. Then the diffeomorphism maps the subset C_0 of R into $\mathbb{R}^4 \natural_\infty X$, where it lies in a compact subset N_0 diffeomorphic to $B^4 \natural_\ell X$ for some ℓ. After pulling N_0 back to $R \natural_\infty X$, we see that it lies in a compact subset of $R \natural_k X$ for some finite $k \geq \ell$. This subset embeds in the required way in an h-cobordism Z between

$E(n)\natural 2\overline{\mathbb{C}P}^2\natural kX$ and $E(n;0)\natural 2\overline{\mathbb{C}P}^2\natural kX$ for some n. As before, there is a product structure over the complement M of intN_0 in $\partial_0 Z$. We lift the 3-sphere $\partial M = \partial N_0$ to obtain a 3-sphere in $\partial_1 Z$ that encloses a compact manifold N_1 lying over N_0. We now have connected sum decompositions $\partial_i Z = \hat{M}\natural\hat{N}_i$ $(i = 0,1)$, where the hats indicate the addition of a 4-handle. Since the manifolds X and $\hat{N}_i$ are negative definite, this contradicts the stability of Donaldson's invariants under summing with negative definite manifolds.   q.e.d.

For R any ribbon $\mathbb{R}^4$ DeMichelis and Freedman [7] show how to construct a naturally nested family $\{R_t|0 \leq t \leq 1\}$ of manifolds homeomorphic to $\mathbb{R}^4$, such that $R_1 = R$, for each t in the standard Cantor set Σ, R_t is a ribbon $\mathbb{R}^4$ with the same ribbon complement C as R, and the remaining manifolds R_t will also be built from C by adding exotic open 2-handles. They show that for suitably constructed R, each diffeomorphism type will have only countably many representatives in the family $\{R_t\}$, so that we obtain uncountably many diffeomorphism types of ribbon $\mathbb{R}^4$'s (with the cardinality of the continuum in ZFC set theory). In fact, their arguments can be adapted to our sequence of nontrivial h-cobordisms, so we obtain a family $\{R_t\}$ as above with R_1 as in Figure 1 (or Figure 3) with each diffeomorphism type represented at most countably many times. (For each $t < 1$, R_t has compact closure in R_1, so embeds as required in some h-cobordism.) Presumably, for each R_t with $t \neq 1$, the engulfing index should be infinite. However, it is possible to use [2] to completely specify each R_t with t in Σ. Each R_t will be built on the ribbon complement of Figure 4 (or Figure 2), and the Casson handle(s) can be assumed to have only one kinky handle at each of the first k stages (for any preassigned k), but at some point the numbers of kinky handles will begin to increase superexponentially.

Relating this to the previous proposition, we obtain a similar family with 2 indices, by setting $R_{s,t} = R_s\natural\bar{R}_t$. For each $s,t \in \Sigma$, $R_{s,t}$ will be an exotic ribbon $\mathbb{R}^4$ with ribbon complement given by the boundary sum of Figure 4 with its mirror image.

Proposition 5.6. *For any $s,t \in I = [0,1]$, there are at most countably many pairs $(s',t') \in I \times I$ for which $R_{s',t'}$ is diffeomorphic to $R_{s,t}$. In fact, there are at most countably many pairs for which $R_{s',t'}$ is both $\mathbb{C}P^2$- and $\overline{\mathbb{C}P}^2$-stably diffeomorphic to $R_{s,t}$.*

Proof.   We generalize the argument of [7] as in [17]. Let $K \subset R_0$

denote the ribbon complement minus a collar of its boundary. For $s, t, s', t' \in I$ with $s < s'$, R_s is canonically embedded with compact closure in $R_{s',t'} \natural_\infty \overline{\mathbb{C}P}^2$. Suppose the latter admits a diffeomorphism onto $R_{s,t} \natural_\infty \overline{\mathbb{C}P}^2$ that restricts to the identity on $K \subset R_s$. Using the obvious embedding $R_t \subset \mathbb{R}^4$ and the compact closure of $R_s \subset R_{s',t'} \natural_\infty \overline{\mathbb{C}P}^2$, we obtain an embedding $d : R_s \hookrightarrow R_s \natural_k \overline{\mathbb{C}P}^2$ for finite k, where $d|K = \mathrm{id}_K$ and $\mathrm{Im}\, d$ has compact closure. As in [17, Lemma 1.2], this allows us to construct negative definite periodic ends and derive a contradiction as in [7]. Thus, no such diffeomorphism exists, and there are at most countably many values s' with some $R_{s',t'}$ $\overline{\mathbb{C}P}^2$-stably diffeomorphic to $R_{s,t}$ (corresponding to different embedding types of K in $R_{s,t} \natural_\infty \overline{\mathbb{C}P}^2$). The same argument with reversed orientation completes the proof.   q.e.d.
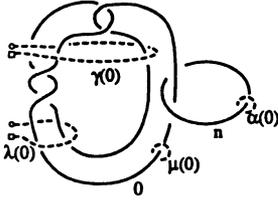
FIGURE 8
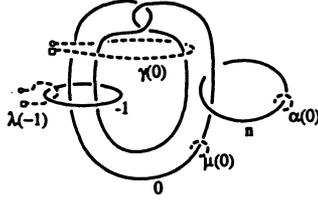
FIGURE 9
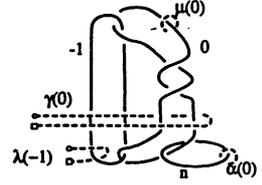
FIGURE 10
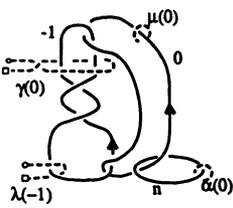
FIGURE 11
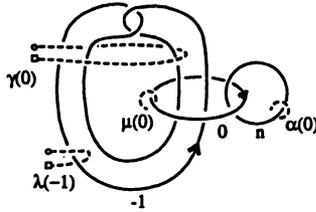
FIGURE 12
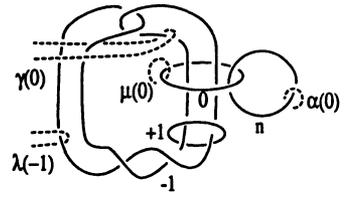
FIGURE 13
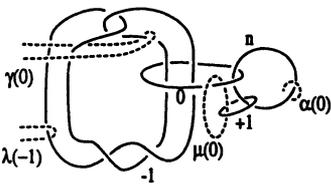
FIGURE 14
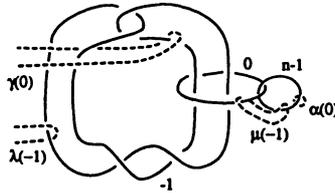
FIGURE 15
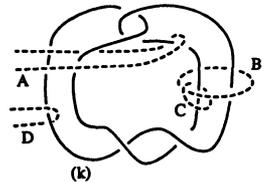
FIGURE 16
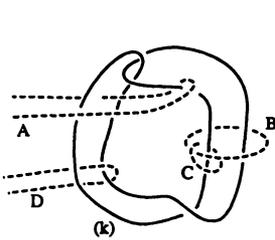
FIGURE 17
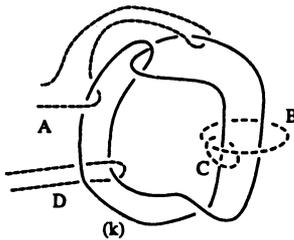
FIGURE 18
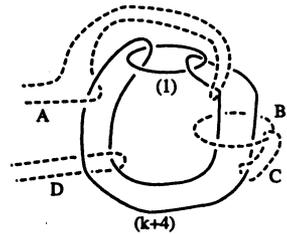
FIGURE 19
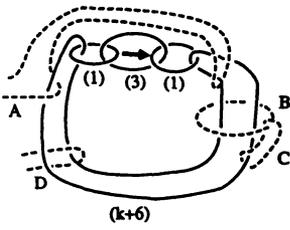
FIGURE 20
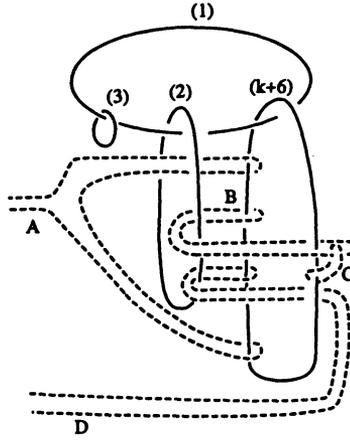
FIGURE 21
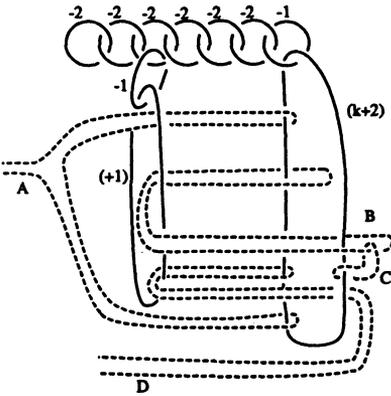
FIGURE 22

FIGURE 23

N_n
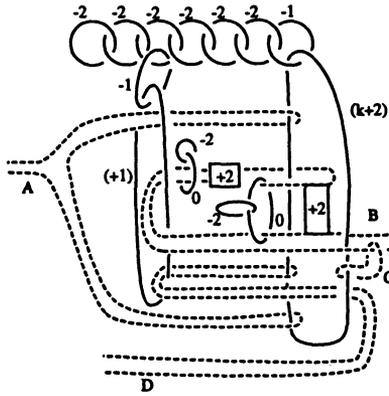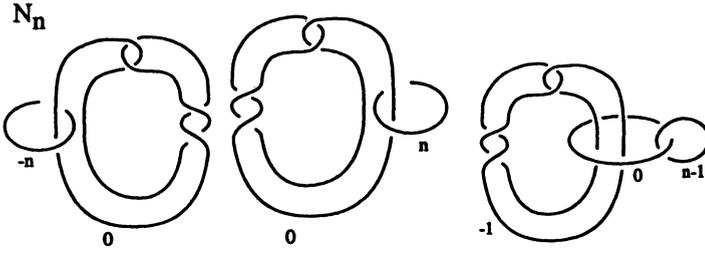
FIGURE 24   FIGURE 25   FIGURE 26

W_n
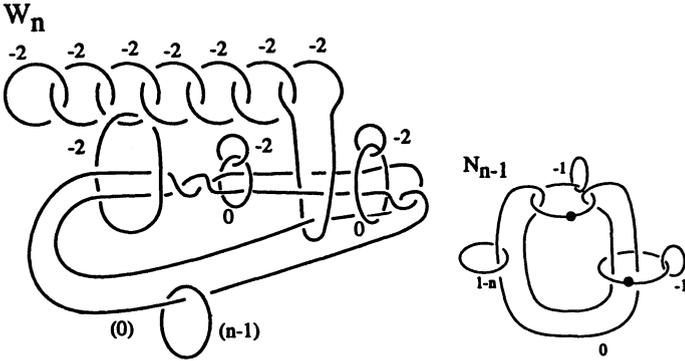
FIGURE 27   FIGURE 28
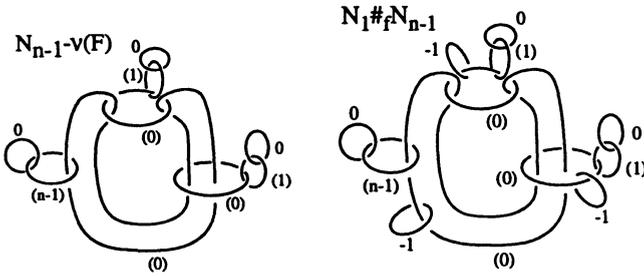
FIGURE 29   FIGURE 30
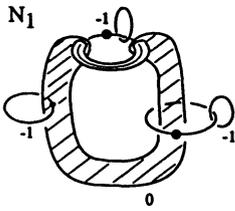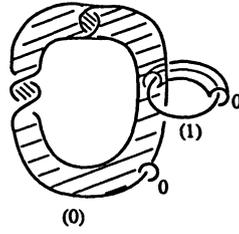
FIGURE 31   FIGURE 32
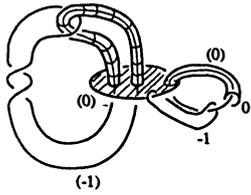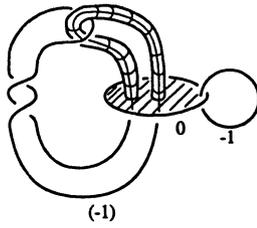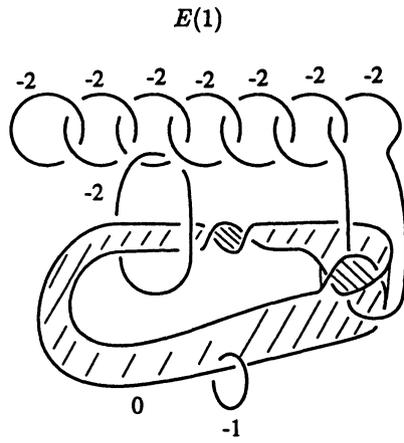
FIGURE 33   FIGURE 34   FIGURE 35

$E(1)$
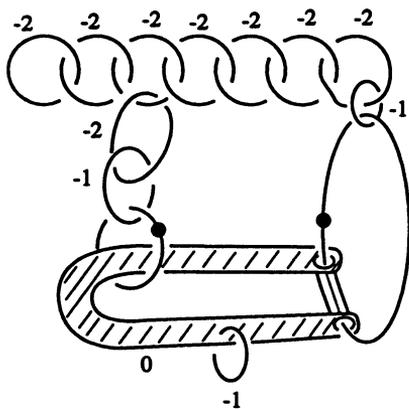
FIGURE 36
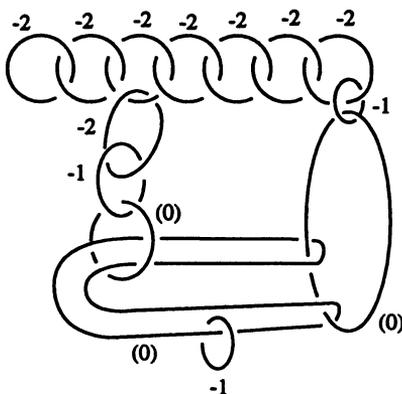
FIGURE 37

FIGURE 38

$E(1) \natural_f N_{n-1}$
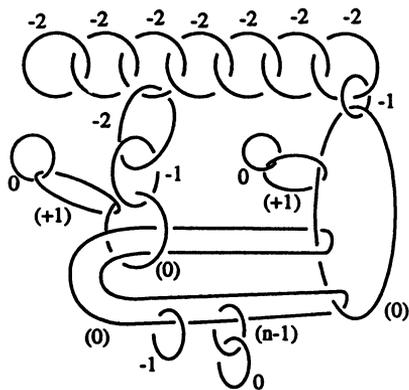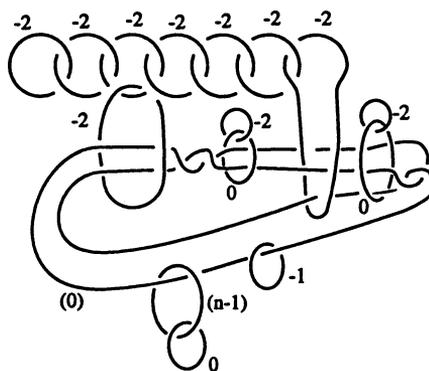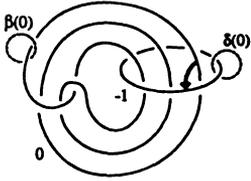
FIGURE 39

FIGURE 40
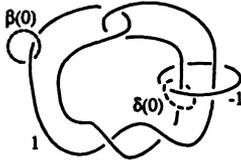
FIGURE 41
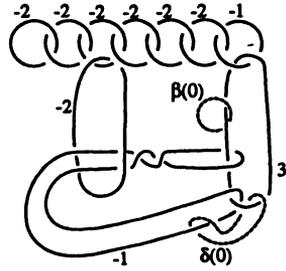
FIGURE 42
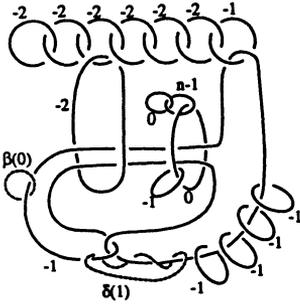
FIGURE 43
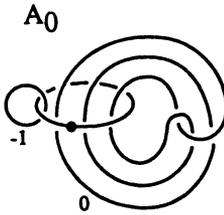
FIGURE 44
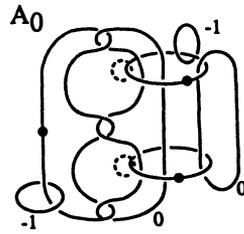
FIGURE 45
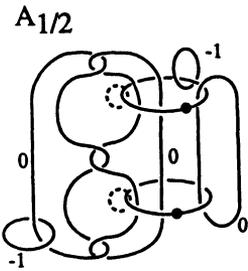
FIGURE 46
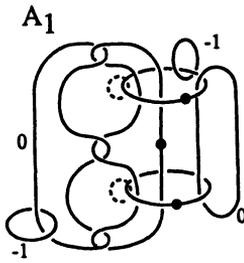
FIGURE 47
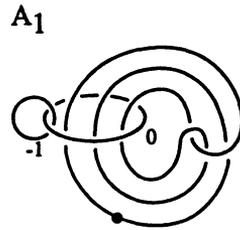
FIGURE 48
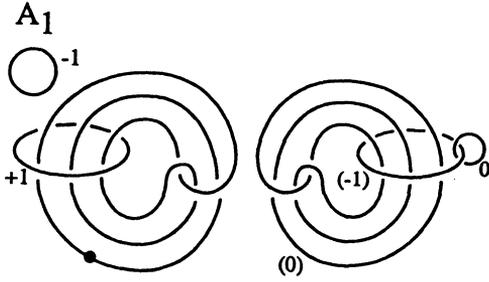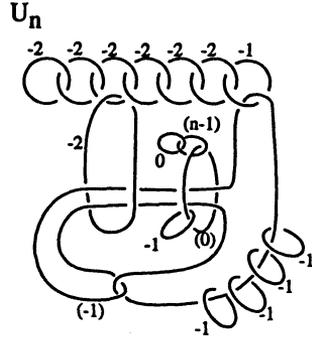
FIGURE 49　　　FIGURE 50　　　FIGURE 51
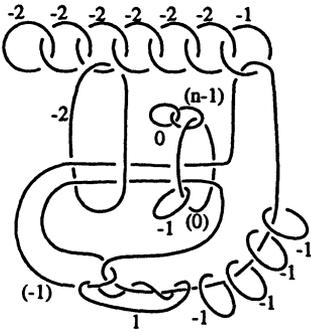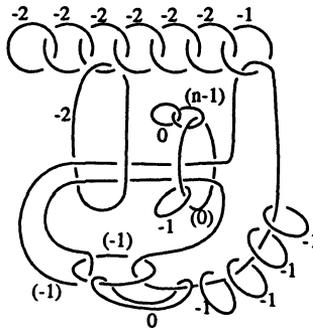
FIGURE 52　　　FIGURE 53
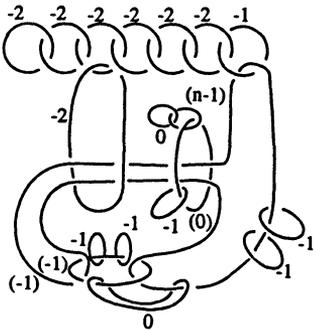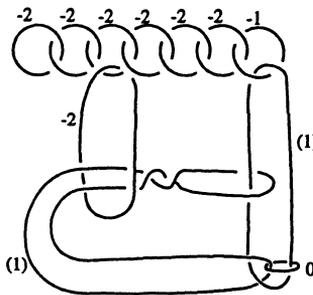
FIGURE 54　　　FIGURE 55
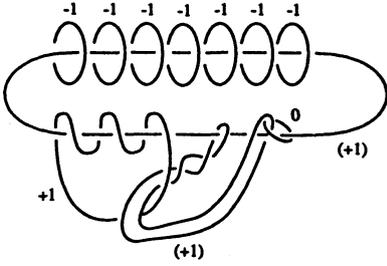
FIGURE 56
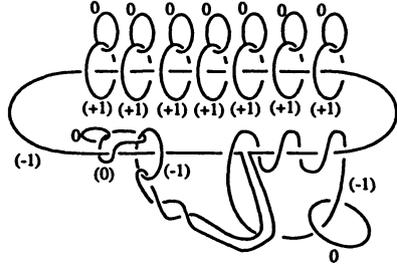
FIGURE 57
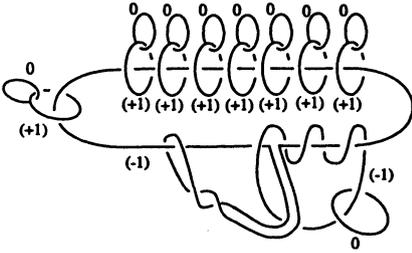
FIGURE 58
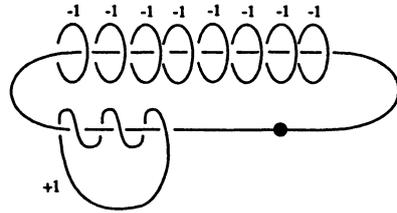
FIGURE 59
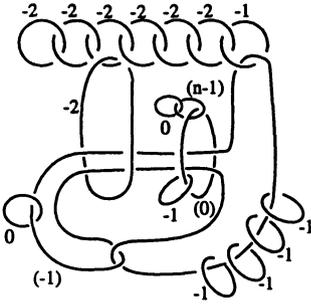
FIGURE 60
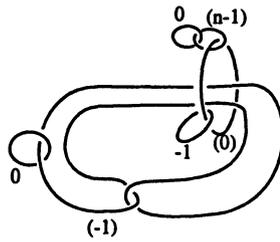
FIGURE 61
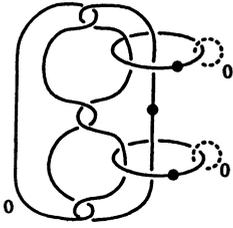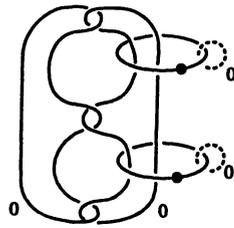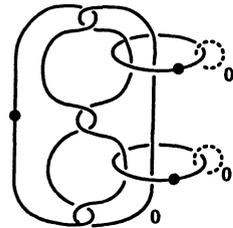
FIGURE 62　　　　FIGURE 63　　　　FIGURE 64
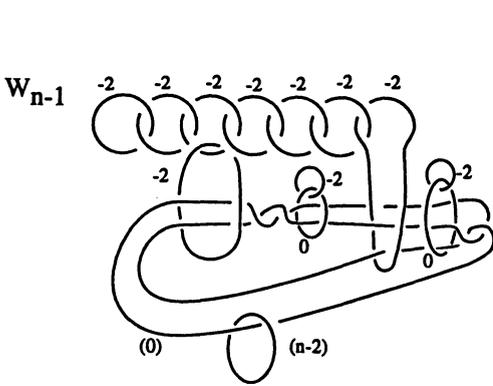
FIGURE 65
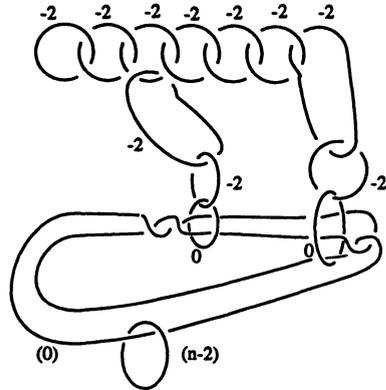
FIGURE 66
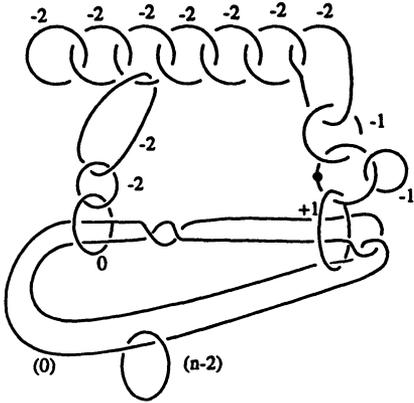
FIGURE 67
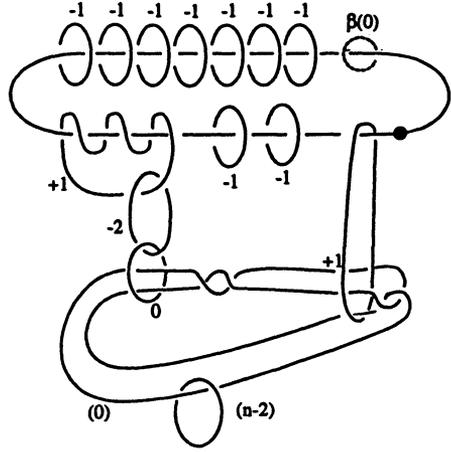
FIGURE 68
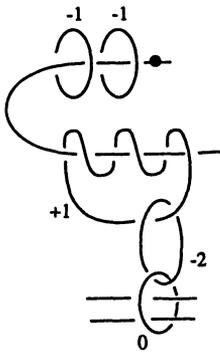
FIGURE 69
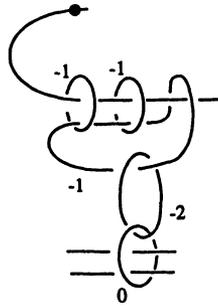
FIGURE 70
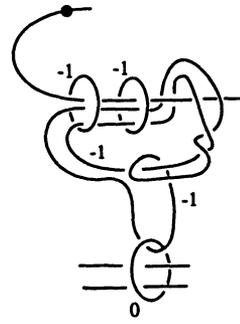
FIGURE 71
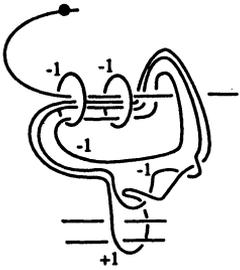
FIGURE 72
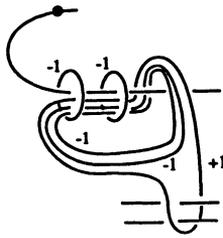
FIGURE 73
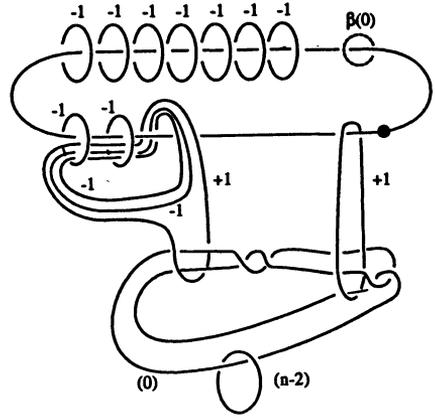
FIGURE 74

$$W_{n-1} \cup_{\phi_{n-2}} W_{n-2}$$
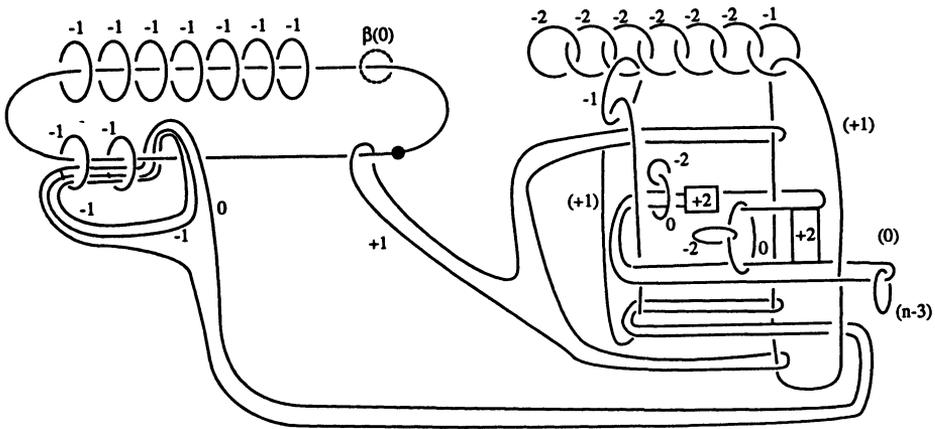
FIGURE 75
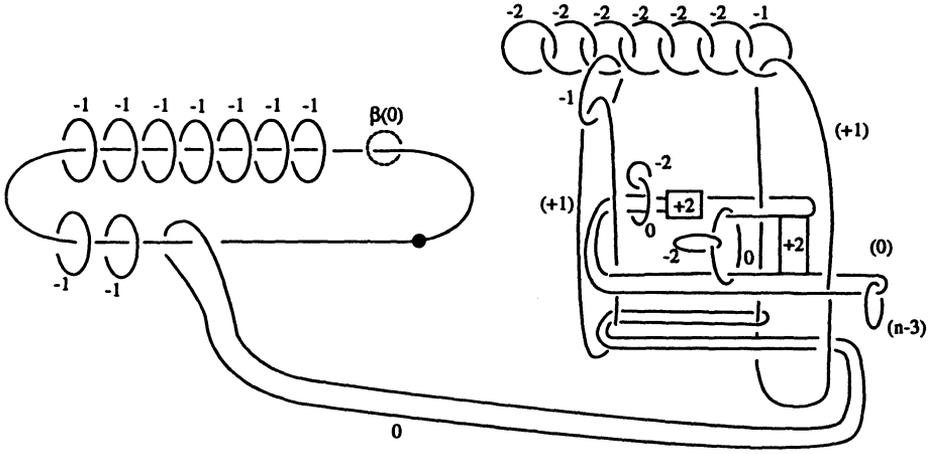
FIGURE 76
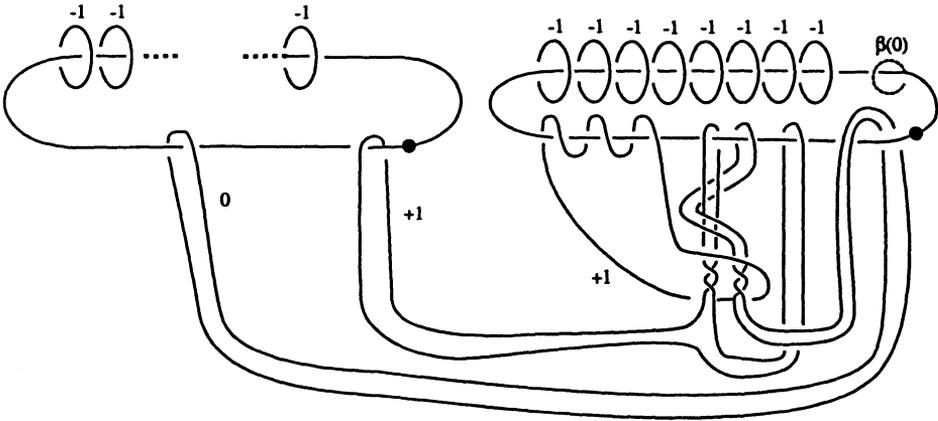
FIGURE 77
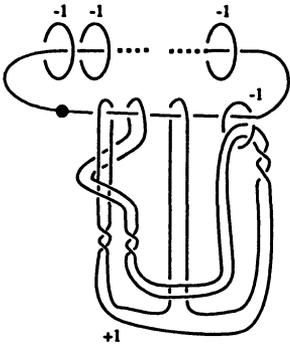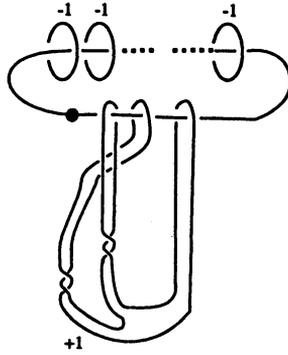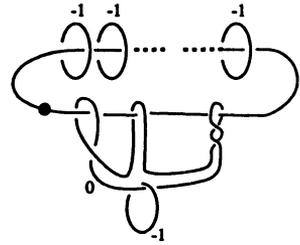
FIGURE 78   FIGURE 79   FIGURE 80
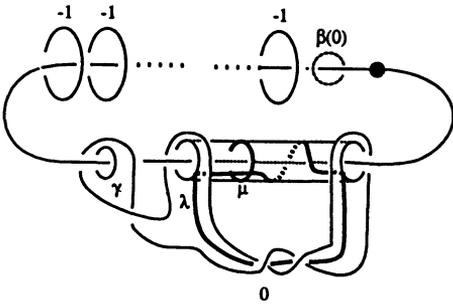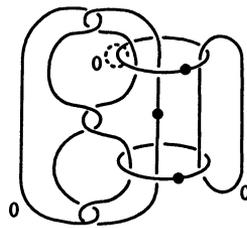
FIGURE 81   FIGURE 82   FIGURE 83

References

[1] S. Akbulut, *A fake compact contractible 4-manifold*, J. Differential Geom. **33** (1991) 335–356.

[2] Ž. Bižaca, *A Reimbedding Algorithm for Casson Handles*, Trans. Amer. Math. Soc. **345** (1994) 435-510.

[3] _____, *A handle decomposition of an exotic* $\mathbb{R}^4$, J. Differential Geom.**39** (1994) 491-508.

[4] _____, *An explicit family of exotic Casson handles*, Proc. Amer. Math.Soc. **123** (1995) 1297-1302.

[5] A. Casson, *Three lectures on new infinite construction in 4-dimensional manifolds*, (notes prepared by L. Guillou), A la Recherche de la Topologie Perdue, L. Guillou & A. Marin, Progress in Mathematics Birkhäuser **62** (1986) 201–244.

[6] T. Cochran & R. Gompf, *Applications of Donaldson's theorems to classical knot concordance, homology 3-spheres and property P*, Topology **27** (1988) 495–512.

[7] S. DeMichelis & M. Freedman, *Uncountably many exotic* R^4's *in standard 4-space*, J. Differential Geom.**35** (1992) 219–254.

[8] S. Donaldson, *Irrationality and the h-cobordism conjecture*, J. Differential Geom.**26** (1987) 141–168.

[9] _____, *Polynomial invariants for smooth four-manifolds*, Topology **29** (1990) 257–315.

[10] S. Donaldson & P. Kronheimer, *The geometry of four-manifolds*, Clarendon Press, Oxford, 1990.

[11] M. Freedman, *The topology of 4-dimensional manifolds*, J. Differential Geom.**17** (1982) 357–453.

[12] R. Friedman & J. Morgan, *On the diffeomorphism types of certain algebraic surfaces, I and II*, J. Differential Geom.**27** (1988) 297–398.

[13] _____, *Smooth four-manifolds and complex surfaces*, Ergeb. Math. 3, No. 27 Springer, Berlin, 1994.

[14] R. Gompf, *An infinite set of exotic R^4's*, J. Differential Geom.**21** (1985) 283–300.

[15] _____, *Nuclei of elliptic surfaces*, Topology **30** (1991) 479–511.

[16] _____, *Sums of elliptic surfaces*, J. Differential Geom. **34** (1991) 93–114.

[17] _____, *An exotic menagerie*, J. Differential Geom.**37** (1993) 199–223.

[18] J. Harer, A. Kas & R. Kirby, *Handlebody decomposition of complex surfaces*, Mem. Amer. Math. Soc. No. 350, 1986.

[19] R. Kirby, *The topology of 4-manifolds*, Lecture Notes in Math. Vol. 1374 Springer, Berlin, 1989

[20] P. Kronheimer & T. Mrowka, *Gauge theory for embedded surfaces, I*, Topology **32** (1993) 773–826.

[21] L. Rudolph, *Quasipositivity as an obstruction to sliceness*, Bull. Amer. Math. Soc. **29** (1993) 51–59.

[22] R. Stern, *Immersed 2-spheres in 4-manifolds*, Lectures for the XI ELAM, Preprint, 1993.

UNIVERSITY OF TEXAS, AUSTIN